Pharmacological Research 216 (2025) 107723

Contents lists available at ScienceDirect

Pharmacological Research

journal homepage: www.elsevier.com/locate/yphrs

Properties of FDA-approved small molecule protein kinase inhibitors: A 2025 update

Robert Roskoski Jr.

Blue Ridge Institute for Medical Research, 221 Haywood Knolls Drive, Hendersonville, NC 28791, United States

ARTICLE INFO

Keywords:
Alopecia areata
Chronic myelogenous leukemia
Epidermal growth factor receptor
Neurofibromatosis
Non-small cell lung cancer, Pediatric glioma

Chemical compounds studied in this article:
Cabozantinib (PubChem CID: 25102847)
Crizotinib (PubChem CID: 11626560)
Deuruxolitinib (PubChem CID: 72704611)
Ensartinib (PubChem CID: 56960363)
Lazertinib (PubChem CID: 121269225)
Mirdametinib (PubChem CID: 9826528)
Tovorafenib (PubChem CID: 25161177)
Imatinib (PubChem CID: 5291)
Sorafenib (PubChem CID: 216239)
Sunitinib (PubChem CID: 5329102)

ABSTRACT

Because of the deregulation of protein kinase action in many inflammatory diseases and cancer, the protein kinase family has become one of the most significant drug targets in the 21st century. There are 85 FDA-approved protein kinase antagonists that target about two dozen different enzymes and four of these drugs were approved in 2024 and a fifth was approved in 2025. Of these drugs, five target dual specificity protein kinases (MEK1/2), fourteen inhibit protein-serine/threonine protein kinases, twenty-one block nonreceptor protein-tyrosine kinases, and 45 target receptor protein-tyrosine kinases. The data indicate that 75 of these drugs are prescribed for the treatment of neoplasms. Seven drugs (abrocitinib, baricitinib, deucravacitinib, deuruxolitinib, ritlecitinib, tofacitinib, upadacitinib) are prescribed for the management of inflammatory diseases (atopic dermatitis, rheumatoid arthritis, psoriasis, alopecia areata, and ulcerative colitis). Of the 85 FDA-approved agents, about two dozen are used in the treatment of multiple diseases. The following four drugs received FDA approval in 2024 – deuruxolitinib (alopecia areata), ensartinib and lazertinib (non-small cell lung cancer), and tovorafenib (pediatric glioma) while mirdametinib was approved in 2025 for the treatment of type I neurofibromatosis (von Recklinghausen disease). Apart from netarsudil, temsirolimus, and trilaciclib, the approved protein kinase blockers are orally bioavailable. This article summarizes the physicochemical properties of all 85 FDA-approved small molecule protein kinase inhibitors including the molecular weight, number of hydrogen bond donors/acceptors, ligand efficiency, lipophilic efficiency, polar surface area, and solubility. A total of 39 of the 85 FDA-approved drugs have a least one Lipinski rule of 5 violation.

1. Overview of therapeutic protein kinase inhibitors

Owing to genetic alterations such as mutations, translocations as well as overexpression, the dysregulation of protein kinase action plays a significant role in the pathogenesis of inflammatory, autoimmune, cardiovascular, and nervous diseases as well as a number of neoplasms. Consequently, these enzymes are among the most important therapeutic targets in the 21st century [1,2]. Between one-fourth and one-third of drug development programs in the United States and throughout the world target protein kinases. The clinical efficacy of imatinib in the management of Philadelphia chromosome-positive CML (chronic myelogenous leukemia), which was approved by the FDA in 2001, prompted the pursuit of orally bioavailable therapeutic protein kinase antagonists [3–5]. This success resulted from the imatinib blockade of the functional chimeric BCR-Abl nonreceptor protein-tyrosine kinase, the causative biochemical lesion that generates these leukemias.

The existence of more than 200 thousand protein kinase X-ray crystal structures in the public domain has played a major role in structure-based drug development. Added to this is a myriad of additional proprietary structures solved by commercial ventures that are widely used

Abbreviations: ALL, acute lymphocytic leukemia; AML, acute myeloid leukemia; AS, activation segment; BP, back pocket; bRo5, beyond Lipinski's rule of five; C-spine, catalytic spine; CS1, catalytic spine residue 1; CML, chronic myelogenous leukemia; CL, catalytic loop; CLL, chronic lymphocytic leukemia; EGFR, epidermal growth factor receptor; FDA, the Food and Drug Administration of the United States; FP, front pocket; GAP, GTPase activating protein; GEF, guanine nucleotide exchange factor; GIST, gastrointestinal stromal tumor; GK, gatekeeper; GPCR, G-protein coupled receptor; GRL, glycine-rich loop; HCC, hepatocellular carcinoma; HTS, high throughput screening; JAK, Janus kinase; KLIFS-3, kinase-ligand interaction fingerprint and structure residue-3; LE, ligand efficiency; LipE, lipophilic efficiency; NSCLC, non-small cell lung cancer; PI3K, phosphatidylinositol 3-kinase; PKA, protein kinase A; PSA, polar surface area; RCC, renal cell carcinoma; Ro5, Lipinski's rule of five; R-spine, regulatory spine; RS1, regulatory spine residue 1; Sh2, shell residue 2; SLL, small lymphocytic lymphoma; TFR, treatment-free remission; VEGFR, vascular endothelial growth factor receptor.

E-mail address: rrj@brimr.org.

https://doi.org/10.1016/j.phrs.2025.107723
Received 29 March 2025; Received in revised form 31 March 2025; Accepted 31 March 2025
Available online 17 April 2025

in drug discovery. More than 400 orally effective typical and atypical protein kinase inhibitors are in clinical trials worldwide [6]. A complete directory of these medicinals, which is regularly updated, can be accessed from www.icoa.fr/pkidb/. There are 85 FDA-approved medicines that target about two dozen different wild-type and mutant protein kinases (Table 1, supplementary material). These two dozen enzymes, however, represent a small portion of the 518-member protein kinase superfamily. Additional drugs directed against these and other protein kinases are in clinical trials worldwide [4–7].

Manning et al. found that the human protein kinase enzyme superfamily contains 478 typical and an additional 40 atypical enzymes [8] including phosphatidylinositol 3-kinase (PI3K) [5,9]. Protein kinases catalyze the following reaction;

$$MgATP^{1-} + protein\text{–}O\text{:}H \rightarrow protein\text{–}O\text{:}PO_3^{2-} + MgADP + H^+$$

Note that the enzyme mediates the transfer of the phosphoryl group or phosphorylium ion ($:PO_3^{2-}$) and not the phosphate group (OPO_3^{2-}). These catalysts are divided into protein-tyrosine kinases (90 members), protein-tyrosine kinase–like enzymes (43), and protein-serine/threonine kinases (385). The protein-tyrosine kinase group consists of both transmembrane receptor (58) and intracellular nonreceptor (32) proteins. Furthermore, the protein-serine/threonine kinase family includes a small group of intracellular enzymes including MEK1/2 that mediate the phosphorylation of both tyrosine and then threonine residues that are found in the activation segment of their target protein kinases. Owing to this distinctive process, MEK1/2 and related enzymes are classified as dual specificity protein kinases. A further indication of the importance of protein kinases is the finding that about one in every 40 human genes (518 protein kinase genes out of an estimated 20,000 human protein-encoding genes) corresponds to a protein kinase. Protein kinases consequently make up about 2.5 % of the human genome. Other data in support of the importance of protein kinases as drug targets is the finding of Manning et al. that 244 protein kinase genes correspond to cancer amplicons and other disease loci [8]. Consequently, as additional research on the pathogenesis of various disorders is performed, it is expected that there will be a significant increase in the number of protein kinase therapeutic targets.

The FDA has approved 85 small molecule therapeutic protein kinase antagonists as of March 2025 (Table 1) [10–15]. Except for netarsudil (an eye drop) and temsirolimus and trilaciclib (which are given intravenously), all kinase blockers are orally bioavailable. Ruxolitinib is a JAK1/2 therapeutic protein kinase antagonist that was approved for the treatment of myelofibrosis and polycythemia vera in 2011. This compound is topically active as a cream and was approved in 2021 for the treatment of atopic dermatitis. Of the 85 approved drugs, forty-six block receptor protein-tyrosine kinases, twenty-one antagonize nonreceptor protein-tyrosine kinases, thirteen inhibit protein-serine/threonine protein kinases, and five block dual specificity protein kinases (MEK1/2) (Table 2). The data show that 75 of the kinase inhibitors are approved for the treatment of solid and nonsolid neoplasms. Furthermore, three of them (belumosudil, ibrutinib, ruxolitinib) are prescribed for the management of graft vs. host disease and three (upadacitinib, tofacitinib, baricitinib) are used for the treatment of rheumatoid arthritis. More than two dozen of these approved medicines are multikinase antagonists. The simultaneous blockade of several protein kinases has potential advantages as well as disadvantages. For instance, the therapeutic efficacy of multikinase inhibitors may be related to the blockade of two or more targets. Cabozantinib and sunitinib, for example, have significant off-target activity against the Axl receptor protein-tyrosine kinase and this action may add to their clinical effectiveness [16]. Contrariwise, the blockade of off-target protein kinases may elicit unwanted side effects. Consequently, we have the problem of whether a magic shotgun multikinase inhibitor should be preferred to Paul Ehrlich's magic bullet [17].

Thirteen of the FDA-approved protein kinase blockers are used for the treatment of nonneoplastic diseases. For example, (i) upadacitinib is employed for the treatment of psoriatic arthritis, rheumatoid arthritis, and atopic dermatitis, (ii) tofacitinib is used for the management of psoriatic arthritis, rheumatoid arthritis, and ulcerative colitis, (iii) baricitinib and upadacitinib are prescribed for the treatment of rheumatoid arthritis, (iv) ruxolitinib and abrocitinib are used for the management of atopic dermatitis, (v) belumosudil, ibrutinib, and ruxolitinib are approved for the treatment of graft vs. host disease, (vi) fostamatinib is prescribed for the management of chronic immune thrombocytopenia, (vii) nintedanib is approved for the treatment of idiopathic pulmonary fibrosis, (viii) deuruxolitinib and ritlecitinib are used for the management of alopecia areata, and (ix) netarsudil is approved for the treatment of glaucoma [10–15]. Additionally, ibrutinib, ruxolitinb, and sirolimus are approved therapeutics for both neoplastic and nonneoplastic diseases.

Eleven of the FDA-approved kinase inhibitors form covalent bonds with their target enzymes and they are accordingly classified as TCIs (targeted covalent inhibitors) [18,19]. These agents include acalabrutinib (blocking BTK in mantle cell lymphoma and CLL), afatinib, dacomitinib, lazertinib, mobocertinib, and osimertinib (all five targeting mutant *EGFR* in NSCLC), neratinib (blocking ErbB2 in HER2-positive breast cancer), zanubrutinib (antagonizing BTK in mantle cell lymphoma), ritlecitinib (blocking JAK3 in alopecia areata), futibatinib (antagonizing FGFR2 fusions or rearrangements in cholangiocarcinomas), and ibrutinib (inhibiting BTK in chronic graft vs. host disease, mantle cell lymphoma, CLL, marginal zone lymphoma, and Waldenström macroglobulinemia). The tightly linked EGFR and ErbB4 of the ErbB1/2/3/4 epidermal growth factor receptor family are the most prevalent protein kinases bearing mutations in all cancers [3]. For a summary of the properties of small molecule protein kinase antagonists that were FDA-approved before 2024, see Refs. [10–15].

Of the 85 FDA-approved protein kinase inhibitors, thirty-three are FDA-approved for the management of more than one disorder. For example, imatinib is approved for the treatment of eight different diseases (Table 2). This agent inhibits the nonreceptor protein-tyrosine kinase Abl (and the BCR-Abl chimera – responsible for the pathogenesis of chronic myelogenous leukemia), Abl2, Kit (the stem cell factor receptor), PDGFRα/β, and epithelial discoidin domain-containing receptor-1 (DDR1) and receptor-2 (DDR2). DDR1/2, which are activated

Table 1
Principal FDA-approved protein kinase inhibitor drug targets[a].

Kinase family	Class of Kinase	US FDA approved
EGFR/ErbB	RY	11
JAK	NRY	10
VEGFR	RY	9
BCR-Abl	NRY	6
ALK	RY	6
FGFR	RY	5
MEK1/2	Y/T	5
B-RAF	S/T	4
BTK	NRY	4
CDK4/6	S/T	4
FKBP	S/T	3
Flt3	RY	3
MET	RY	3
RET	RY	2
ROCK	S/T	2
TRKA	RY	2
CSF1	RY	1
Kit	RY	1
PDGFR	RY	1
ROS1	RY	1
SYK	RY	1
TYK2	NRY	1
Total		85

[a] NYR, nonreceptor protein-tyrosine kinase; RY, receptor protein-tyrosine kinase; S/T, protein-serine/threonine kinase; Y/T, Dual specificity protein kinase – tyrosine phosphorylation followed by threonine phosphorylation of target kinase activation segments.

Table 2
FDA-approved small molecule protein kinase inhibitors, their protein kinase targets, and therapeutic indications[a].

Drug	Code	Company	Trade name	Year approved	Primary targets[b]	Therapeutic indications[c]
Abemaciclib	LY2835219	Lilly	Verzenio	2017	CDK4/6	$HER2^+$ breast cancer, both monotherapy and combination therapy
Abrocitinib	PF04965842	Pfizer	Cibinqo	2022	JAK1	Atopic dermatitis in adults and children 12 years of age and older
Acalabrutinib	ACP−196	Acerta Pharma	Calquence	2017	BTK	Mantle cell lymphoma, chronic lymphocytic leukemia (CLL), small lymphocytic lymphoma (SLL)
Afatinib	BIBW2992	Boehringer Ingelheim	Tovok	2013	ErbB1/2/4	NSCLC (non-small cell lung cancer) and squamous NSCLC
Alectinib	CH5424802	Roche	Alecensa	2015	ALK, RET	ALK^+ NSCLC
Asciminib	ABL001	Novartis	Scemblix	2021	BCR-Abl	First or second-line treatment of Ph^+ CML with or without a T315I mutation
Avapritinib	BLU285	Blueprint Medicines	Ayvakit	2020	PDGFRα	Gastrointestinal stromal tumors (GIST) with a *PDGFRα* exon 18 mutations; indolent and advanced systemic mastocytosis
Axitinib	AG013736	Pfizer	Inlyta	2012	VEGFR1/2/3	Single agent and combination therapy for renal cell carcinoma (RCC)
Baricitinib	LY3009104	Lilly	Olumiant	2018	JAK1/2	Rheumatoid arthritis
Belumosudil	KD025	Kadmon Pharma	Rezurock	2021	ROCK2	Graft vs. host disease in adults and pediatric patients 12 years of age and older
Binimetinib	MEK162	Array BioPharma	Mektovi	2018	MEK1/2	Melanoma with *BRAF V600E/K* and NSCLC with *BRAF* V600E mutations with encorafenib
Bosutinib	SKI−606	Pfizer	Bosulif	2012	BCR-Abl	Ph^+ CML
Brigatinib	AP 26113	Ariad Pharm	Alunbrig	2017	ALK	ALK^+ NSCLC
Cabozantinib	BMS907351	Exelixis	Cometriq & Cabometyx	2012	RET, VEGFR2	Differentiated thyroid cancer, RCC, HCC
Capivasertib	AZD5363	AstraZeneca	Truqap	2023	HER2	Hormone receptor (HR)-positive, human epidermal growth factor receptor 2 (HER2)-negative breast cancer bearing *PIK3CA/AKT1/PTEN* mutations
Capmatinib	INC280	Novartis	Tabrecta	2020	MET (HGFR)	NSCLC with *MET* exon 14 skipping mutations
Ceritinib	LDK378	Novartis	Zykadia	2014	ALK	ALK^+ NSCLC
Cobimetinib	GDC−0973	Genentech	Cotellic	2015	MEK1/2	$BRAF^{V600E/K}$ melanomas in combination with vemurafenib; histiocytic neoplasms
Crizotinib	PF2341066	Pfizer	Xalkori	2011	ALK, ROS1	ALK^+ (i) NSCLC,(ii) anaplastic large cell lymphoma, (iii) inflammatory myofibroblastic tumors, (iv) anaplastic large cell lymphoma; $ROS1^+$ NSCLC
Dabrafenib	GSK2118436	GSK	Tafinlar	2013	B-Raf	*BRAF* mutation-positive (i) melanomas (V600K/E), (ii) NSCLC (V600E), (iii) anaplastic thyroid cancers (V600E); pediatric glioma (V600E)
Dacomitinib	PF00299804	Pfizer	Visimpro	2018	EGFR	*EGFR*-mutant NSCLC with an exon 19 deletion or exon 21 L858R substitution
Dasatinib	BMS354825	Bristol Myers Squibb	Sprycel	2006	BCR-Abl	Ph^+ CML or ALL
Deucravacitinib	BMS986165	Bristol Myers Squibb	Sotyktu	2022	TYK2	Psoriasis
Deuruxolitinib	CTP−543	Sun Pharmaceutical Industries, Inc.	Leqselvi	2024	JAK2/1	Alopecia areata
Encorafenib	LGX818	Array BioPharma	Braftovi	2018	B-Raf	*BRAF* mutant melanoma (V600E/K) or NSCLC (V600E) in combination with binimetinib; *BRAF* mutant colorectal cancer (V600E) in combination with cetuximab
Ensartinib	LGX818	Xcovery Holdings, Inc.	Ensacove	2024	ALK	First-line treatment of ALK^+ NSCLC
Entrectinib	RXDX101	Genentech	Rozlytrek	2019	TRKA/B/C, ROS1	Solid tumors with NTRK fusion proteins, $ROS1^+$ NSCLC
Erdafitinib	JNJ42756493	Jansen Pharm	Balversa	2019	FGFR1/2/3/4	Second-line treatment of urothelial bladder cancer with *FGFR3* gene alterations
Erlotinib	OSI−774	Genentech	Tarceva	2004	EGFR	NSCLC, pancreatic cancer
Everolimus	RAD001	Novartis	Afinitor	2009	FKBP12/mTOR	HER2-negative breast cancer, pancreatic neuroendocrine tumors, RCC, renal angiomyolipoma, subependymal giant cell astrocytoma
Fedratinib	TG101348	Celgene	Inrebic	2019	JAK2	Primary or secondary myelofibrosis
Fostamatinib	R788	Rigel Pharma.	Tavalisse	2018	Syk	Chronic immune thrombocytopenia
Fruquintinib	HMPL013	Takeda	Fruzaqla	2023	VEGFR2	CRC
Futibatinib	TAS120	Tiaho Pharma	Lytgobi	2022	FGFR2	Bile duct cancers (cholangiocarcinomas) with FGFR2 fusion proteins or other rearrangements
Gefitinib	ZD1839	AstraZeneca	Iressa	2003	EGFR	NSCLC with exon 19 deletions or exon 21 L848R substitutions
Gilteritinib	ASP2215	Astellas Pharma	Xospata	2018	Flt3	*FLT3*-mutation positive AML
Ibrutinib	PCI−32765	Johnson & Johnson	Imbruvica	2013	BTK	CLL,SLL, graft vs. host disease, Waldenström macroglobulinemia
Imatinib	STI571	Novartis	Gleevec	2001	BCR-Abl	Ph^+ CML or ALL, aggressive systemic mastocytosis, chronic eosinophilic leukemia, dermatofibrosarcoma protuberans, hypereosinophilic syndrome, GIST, myelodysplastic/myeloproliferative disease
Infigratinib	BGJ398	QED Therapeutics	Truseltiq	2021	FGFR2	Cholangiocarcinomas with FGFR2 fusions or other rearrangement
Lapatinib	GW572016	GSK	Tykerb	2007	EGFR, ErbB2/HER2	$HER2^+$ breast cancer in combination with capecitabine or letrozole

(*continued on next page*)

Table 2 (*continued*)

Drug	Code	Company	Trade name	Year approved	Primary targets[b]	Therapeutic indications[c]
Larotrectinib	LOXO−101	Bayer	Vitrakvi	2018	TRKA/B/C	Solid tumors with NTRK fusion proteins
Lazertinib	GNS1480	Janssen Biotech, Inc.	Lazcluze	2024	Mutant *EGFR*	NSCLC with exon19 deletions or exon 21 L858R substitutions in combination with amivantamab
Lenvatinib	AK175809	Easai Co.	Lenvima	2015	VEGFR, RET	Differentiated thyroid cancer, HCC, RCC, endometrial carcinoma
Lorlatinib	PF06463922	Pfizer	Lorbrena	2018	ALK	ALK^+ NSCLC
Midostaurin	CPG 41251	Novartis	Rydapt	2017	Flt3	*FLT3* mutation positive AML, mastocytosis, mast cell leukemia
Mirdametinib	PD0325901	SpringWorks Therapeutics, Inc.	Gomekli	2025	MEK1/2	Type I neurofibromatosis
Mobocertinib	TAK−788	Takeda Pharm.	Exkivity	2021	EGFR	NSCLC with *EGFR*-positive exon 20 insertions
Momelotinib	CYT 387	GSK	Ojjaara	2023	JAK1/2	Primary or secondary myelofibrosis patients with anemia
Neratinib	HKI−272	Puma Biotech	Nerlynx	2017	ErbB2/ HER2	Second and third-line treatment of $HER2^+$ breast cancer
Netarsudil	AR11324	Aerie Pharma	Rhopressa	2018	ROCK1/2	Glaucoma
Nilotinib	AMN107	Novartis	Tasigna	2007	BCR-Abl	First or second-line treatment of Ph^+ CML
Nintedanib	BIBF−1120	Boehringer Ingelheim	Vargatef	2014	FGFR1/2/3	Idiopathic pulmonary fibrosis, chronic fibrosing interstitial lung diseases
Osimertinib	AZD−9292	AstraZeneca	Tagrisso	2015	EGFR	NSCLC with exon 19 deletions, exon 21 substitutions (L858R), or T790M mutations
Pacritinib	SB1518	CTI BioPharma	Vonjo	2022	JAK2	Primary or secondary myelofibrosis with a low platelet count
Palbociclib	PD0332991	Parke-Davis	Ibrance	2015	CDK4/6	HR^+ and $HER2^-$ breast cancer in combination with (i) an aromatase inhibitor or (ii) fulvestrant
Pazopanib	GW786034	GSK	Votrient	2009	VEGFR1/2/ 3	RCC, soft tissue sarcomas
Pemigatinib	INCB054828	Incyte Corp.	Pemazyre	2020	FGFR2	Advanced cholangiocarcinoma with a FGFR2 fusions or rearrangements
Pexidartinib	PLX3397	Plexxikon Inc	Turalio	2019	CSF1R	Tenosynovial giant cell tumors
Pirtobrutinib	LOXO−305	Lilly	Jaypirca	2023	BTK	Mantle cell lymphoma, CLL, SLL
Ponatinib	AP 24534	Ariad Pharm	Iclusig	2012	BCR-Abl	Ph^+ ALL, CML, $T315I^+$ CML
Pralsetinib	Blu−667	Blueprint Medicines	Gavreto	2020	RET	RET-fusion protein NSCLC, RET- fusion protein thyroid cancer
Quizartinib	ASP−2869	Daiichi Sankyo	Vanflyta	2023	Flt3	*FLT3* internal tandem duplication positive AML in combination with cytarabine and daunorubicin
Regorafenib	BAY 734506	Bayer	Stivarga	2012	VEGFR1/2/ 3	Second-line treatment of CRC, HCC, GIST
Repotrectinib	TX−0005	Bayer	Augtyro	2023	ROS1	$ROS1^+$ NSCLC and solid tumors with neurotrophic tyrosine receptor kinase (NTRK) gene fusion
Ribociclib	LEE011	Novartis	Kisqali	2017	CDK4/6	HR^+ /$HER2^-$ breast cancer combination therapy
Ripretinib	DCC−2618	Decipera Pharma.	Qinlock	2020	Kit, PDGFRα	Fourth-line treatment of GIST
Ritlecitinib	PF06651600	Pfizer	Litfulo	2023	JAK3	Alopecia areata
Ruxolitinib	INCB018424	Incyte Corp.	Jakafi	2011	JAK1/2/3, Tyk	Myelofibrosis, polycythemia vera, graft vs. host disease, atopic dermatitis (applied topically)
Selpercatinib	CEGM9YBNG	Lilly	Retevmo	2020	RET	RET fusion (i) NSCLC, (ii) solid tumors and (iii) thyroid cancers; *RET* mutant medullary thyroid cancer
Selumetinib	AZD6224	AstraZeneca	Koselugo	2020	MEK1/2	Type I neurofibromatosis
Sirolimus	AY 22989	Wyeth, LLC	Rapamycin	1999	FKBP12/ mTOR	Kidney transplant, lymphangioleiomyomatosis
Sorafenib	BAY 439006	Bayer	Nexavar	2005	VEGFR1/2/ 3	HCC, RCC, differentiated thyroid cancer
Sunitinib	SU11248	Pfizer	Sutent	2006	VEGFR2	GIST, RCC, pancreatic neuroendocrine tumors
Temsirolimus	CCI−779	Wyeth, LLC	Torisel	2007	FKBP12/ mTOR	RCC
Tepotinib	EMD1214063	EMD Serono Inc.	Tepmetko	2021	MET (HGFR)	NSCLC with *MET*-exon skipping alterations
Tivozanib	AV951	AVEO Pharma	Fotvida	2021	VEGFR2	Third-line treatment of RCC
Tofacitinib	CP−690550	Pfizer	Tasocitinib	2012	JAK3	Rheumatoid, psoriatic, and juvenile idiopathic arthritis, ulcerative colitis, ankylosing spondylitis
Tovorafenib	DAY101	Pfizer	Ojemda	2024	B-/C-Raf	Pediatric low grade glioma in patients older than six months harboring a *BRAF* fusion or rearrangement or a *BRAF* V600 mutation
Trametinib	GSK1120212	GSK	Mekinist	2013	MEK1/2	Melanoma with *BRAF V600E* or *V600K* mutations with dabrafenib; NSCLC, anaplastic thyroid cancer, and low grade glioma in children with *BRAF* V600E mutations with dabrafenib
Trilaciclib	G1T28	G1 Therapeutics	Cosela	2021	CDK4/6	Chemotherapy-induced myelosuppression when administered prior to a cytotoxic regimen for small cell lung cancer
Tucatinib	ONT−380	Seattle Genetics	Tukysa	2020	ErbB2/ HER2	$HER2^+$ breast cancer, CRC
Upadacitinib	ABT−494	AbbVie	Rinvoq	2019	JAK1	Second-line treatment for rheumatoid arthritis, psoriatic arthritis, atopic dermatitis, ulcerative colitis
Vandetanib	ZD6474	Sanofi	Zactima	2011	RET	Medullary thyroid cancer
Vemurafenib	PLX−4032	Genentech	Zelboraf	2011	B-Raf	*BRAF V600E* mutation positive melanoma, *BRAF V600* Chester-Erdheim disease
Zanubrutinib	BGB3111	BeiGene	Brukinsa	2019	BTK	Mantle cell lymphoma, Waldenström macroglobulinemia, marginal zone lymphoma, CLL, SLL, follicular lympmphoma

[a] Data from Refs. [10–13].

[b] Although many of these drugs are multikinase inhibitors, only the primary therapeutic targets are given here.

[c] ALK$^+$, ALK-positive; ALL, acute lymphoblastic leukemias; AML, acute myelogenous leukemias; CLL, chronic lymphocytic leukemia; CML, chronic myelogenous leukemia; ErbB2/HER2, human epidermal growth factor receptor-2; GIST, gastrointestinal stromal tumor; HCC, hepatocellular carcinoma; HER2$^+$, human epidermal growth factor receptor-2 positive; HR$^+$, hormone receptor positive; MET (HGFR), hepatocyte growth factor receptor; NSCLC, non-small cell lung cancer; Ph$^+$, Philadelphia chromosome positive; RCC, renal cell carcinoma; SLL, small lymphocytic lymphoma.

by collagen, participate in cell migration, differentiation, proliferation, and extracellular matrix remodeling. Imatinib is prescribed for (i) the first-line treatment of Philadelphia chromosome-positive chronic myelogenous leukemia, (ii) acute lymphoblastic leukemia, (iii) myelodysplastic/myeloproliferative diseases with *PDGFR* gene-rearrangements, (iv) *KIT* mutation-positive gastrointestinal stromal tumors, (v) chronic eosinophilic leukemia, (vi) hypereosinophilic syndrome, (vii) dermatofibrosarcoma protuberans, and (viii) as a second-line treatment for aggressive systemic mastocytosis without the *KIT* ^{D816V} mutation [2,10]. Moreover, imatinib is used off-label for the treatment of chronic myelogenous leukemia following allogeneic stem cell transplantation, advanced *KIT*-mutant melanomas, chordomas, and desmoid tumors. Consequently, imatinib is a bona fide broad-spectrum inhibitor.

2. The structure and mechanism of protein kinases

2.1. Primary, secondary, and tertiary structures

Because the newly approved drugs described in this article interact with (i) the nonreceptor protein tyrosine kinases JAK1/2, (ii) the protein-serine/threonine kinase B-Raf, (iii) the ALK and EGFR transmembrane receptor protein-tyrosine kinases, and (iv) the MEK1/2 dual specificity protein kinase, the following description is general. As described initially for protein kinase A (PKA) by Knighton et al., phosphoprotein transferases have a small N-terminal lobe and large C-terminal lobe (Fig. 1A) [20]. The amino-terminal lobe consists of a five-stranded antiparallel β-sheet (β1–β5) (Fig. 1A) [20,21]. The N-lobe includes a glycine-rich loop (GRL), also called the P-loop (for the ATP phosphates), which connects the β1- and β2-strands of the amino-terminal lobe (Fig. 1C); the loop consists of GxGxΦG – the Φ is usually a hydrophobic residue. A canonical valine residue two residues after the G-rich loop interacts hydrophobically with the adenine base of ATP and numerous small molecule protein kinase blockers. Protein kinases have an AxK sequence within the amino-terminal β3-strand and a constant glutamate near the center of the αC-helix. A salt bridge links the cationic β3-strand lysine (K) and the anionic αC-glutamate (E) in functional protein kinases and such structures correspond to an "αC_{in}" conformation (Fig. 1A/C). The αC_{in} structure is necessary, but not sufficient, for the manifestation of full catalytic activity. Moreover, enzymes lacking this salt bridge are catalytically inactive and such structures represent the "αC_{out}" conformation (Fig. 1E). The conversion of the αC_{out} to the αC_{in} configuration is necessary for the attainment of

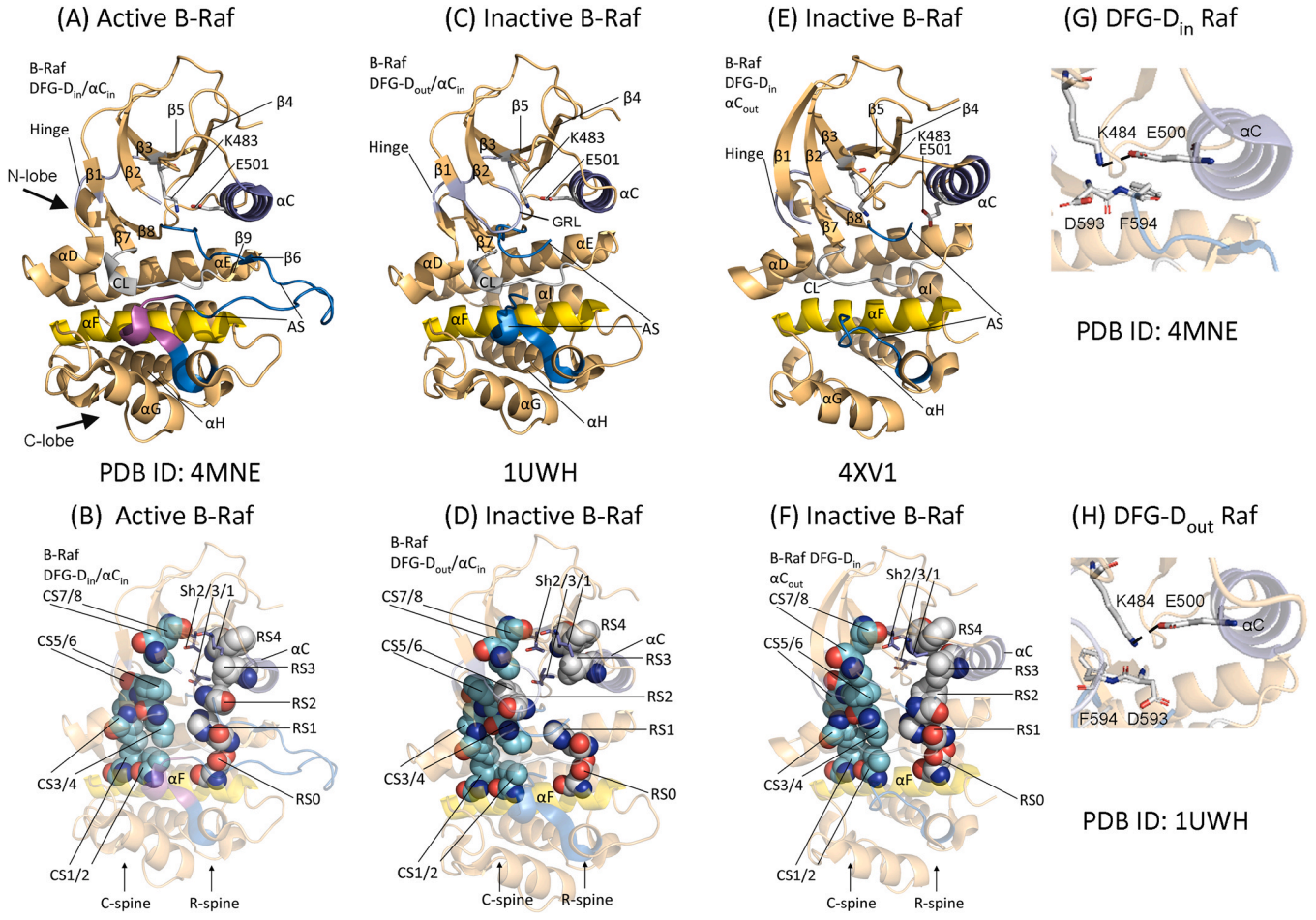

Fig. 1. (A) Overview of active B-Raf and (B) its C-spine, R-spine, and shell residues. (C) The DFG-D_{out} and αC_{in} structure of dormant B-Raf and (D) its C-spine, R-spine, and shell residues. (E) Overview of the DGF-D_{in} and αC_{out} structure of B-Raf and (F) its C-spine, R-spine, and shell residues. (G) The DFG-D_{in} conformation. (H) The DFG-D_{out} conformation. AS, activation segment; CL, catalytic loop. GRL, glycine-rich loop. Fig. 1, 2, 5, and 8 were prepared using the PyMOL Molecular Graphics System Version 2.5.4 Schrödinger, LLC.

maximum catalytic activity.

The C-terminal lobe is mainly α-helical (Fig. 1C) with six conserved helices (αD–αI) [22]. The large lobe of catalytically competent protein kinases contains four small β-strands (β6–β9) (Fig. 1A). The second amino acid in the β7-strand represents the floor of the adenine binding pocket, and this residue makes hydrophobic contact with all known ATP-competitive protein kinase inhibitors [23]. The large lobe contains a catalytic loop (CL) that catalyzes the transfer of the γ-phosphoryl group from ATP to its protein substrates. The carboxyterminal lobe also selects and positions the protein substrate into the active site to facilitate catalysis.

Hanks and Hunter described a dozen subdomains (I–VIa, VIb–XI) that constitute the operational modules of protein kinases [24]. A K/E/D/D (Lys/Glu/Asp/Asp) tetrad performs an indispensable role in the catalytic action of protein kinases. The *K* of the tetrad is the β3-strand lysine that forms salt bridges with the α-phosphate and β-phosphate of ATP as well as the αC-glutamate forming the αC_{in} structure. The kinase activation segment positions the phosphorylatable protein substrate into the active site. Furthermore, the HRD-D of the catalytic-loop (the first *D* of the K/E/*D*/D tetrad) acts as a Lowry-Brönsted base (a proton acceptor). Madhusudan et al. proposed that the catalytic loop HRD-D abstracts the proton from the protein substrate –OH [25]. Moreover, Zhou and Adams suggested that the HRD-D positions the protein substrate –OH group to enable the in-line nucleophilic attack of the oxygen with the γ-phosphoryl group of ATP (Fig. 2) [26]. See Ref. [27] for an explication of protein kinase enzymology and see Table 3 for a list of the essential residues of the main protein kinases considered in this article.

The second *D* of the K/E/D/*D* tetrad is the initial residue of the protein kinase activation segment (AS). This segment of all protein kinases begins with DFG and ends with APE or a similar triad such as PPE or SPE. Activation segments, which vary from about 33–44 residues, are important structural and regulatory components of all protein kinases [28]. An $HRD(x)_4N$ canonical signature comprises the catalytic loop of functional protein kinases. The AS is found C-terminal to the catalytic loop. Two Mg^{2+} ions – $Mg^{2+}(1)$ and $Mg^{2+}(2)$ – are essential for the activity of most, but not all, protein kinases. $Mg^{2+}(1)$ interacts with the activation segment DFG-D and $Mg^{2+}(2)$ interacts with the terminal catalytic loop asparagine (Fig. 2).

The primary structure and length of the middle portion of the activation segment vary considerably in the protein kinase superfamily [2]. The AS of all protein kinases contains one or more phosphorylatable residues. Furthermore, AS phosphorylation is necessary for the expression of maximal enzyme activity of nearly all protein kinases. ErbB1/2/4 of the EGFR family and Flt3 are exceptions because they display maximal activity without AS phosphorylation. The protein kinase activation segment DFG occurs close to the conserved catalytic loop HRD sequence and the αC-helix. The regulatory αC-helix, which occurs within the amino-terminal lobe, nonetheless is found in a strategically important location between the two lobes. The activation segment of protein kinases has an open and extended structure in the active form of all protein kinases (Fig. 1A) and a closed structure in most inactive enzymes (not shown in Fig. 1C/E owing to disorder) [2]. The first two AS residues occur in different conformations. The DFG-D side chain of functional enzymes is directed inward toward the ATP-binding site and it binds $Mg^{2+}(1)$. This configuration is called the "$DFG\text{-}D_{in}$" conformation (Fig. 1G). The DFG-D side chain in many dormant protein kinases is directed away from the ATP-binding site. Such configurations are known as the "$DFG\text{-}D_{out}$" conformation (Fig. 1H). It is the ability of DFG-D to interact ($DFG\text{-}D_{in}$) or to not interact ($DFG\text{-}D_{out}$) with $Mg^{2+}(1)$ within the active site that is of importance.

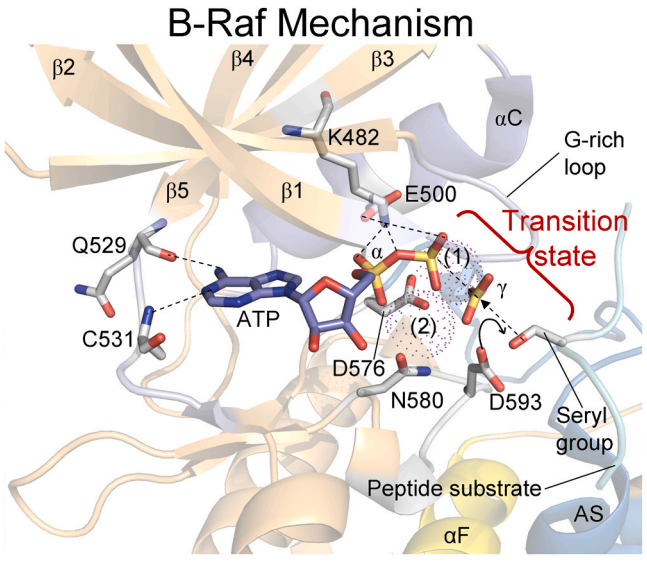

Fig. 2. Postulated mechanism of B-Raf mediated phosphorylation of MEK1. Adapted and derived from PDB ID: 3qhr.

Modi and Dunbrack studied the interaction of drugs and ligands with active and inactive configurations of protein kinases based upon the conformation of the activation segment, which begins with the conserved DFG sequence [29,30]. With $DFG\text{-}D_{in}$, the phenylalanine residue interacts with the αC-helix of the amino-terminal lobe; with $DFG\text{-}D_{out}$, the phenylalanine occurs in a portion of the physiological ATP-binding site thereby creating an αC-helix pocket. These investigators found a group of protein kinase structures that depend upon the position of the phenylalanine side chain ($DFG\text{-}D_{in}$, $DFG\text{-}D_{out}$, and $DFG\text{-}D_{intermediate}$) and the backbone dihedral angles of the xDF sequence (x is the residue before DFG). These authors found eight different arrangements and classified them based upon the conformation (χ1) of the phenylalanine rotamer (plus, minus, trans) and on the Ramachandran regions (A, alpha; B, beta; L, left) of the xDF motif. Their groupings divide the $DFG\text{-}D_{in}$ configuration into six clusters including BLAminus, which represents an active structure as well as two prevalent inactive forms, ABAminus and BLBplus. $DFG\text{-}D_{out}$ assemblies occur chiefly in the BBAminus configuration. The inactive enzymes possess features that impede their interaction with ATP, Mg^{2+}, and/or their protein substrates. Modi and Dunbrack created a useful searchable and noncommercial web site (http://dunbrack3.fccc.edu/kincore/) that allows one to determine whether a given protein kinase structure corresponds to an active or inactive enzyme. We used this web site to determine whether the structures of our various drug-enzyme combinations correspond to active ($DFG\text{-}D_{in}$, BLAminus) or inactive (otherwise) enzymes.

2.2. The hydrophobic skeletons and associated shell residues of protein kinases

Kornev et al. investigated the three-dimensional structures of active and inactive conformations of about two dozen protein kinases to identify structurally critical residues [31,32]. Their analysis uncovered a quartet of four amino acids that make up a regulatory spine (R-spine) an octet of eight amino acids along with the adenine base of ATP that make up a catalytic spine (C-spine). These residues occur in both the N-terminal and C-terminal lobes. These spines generate a stable, but flexible, catalytically competent entity. The C-spine includes ATP and the R-spine helps to localize the protein substrate for catalysis. The R-spine contains components of both the αC-helix and the activation segment, whose structures are vital in determining active and inactive enzyme states. The precise positioning and alignment of each spine are necessary, but not sufficient, for the formation of a catalytically competent protein kinase.

The R-spine contains the initial amino acid of the β4-strand along with the amino acid that is four residues carboxyterminal to the conserved αC-helix glutamate, both of which are within the N-terminal lobe [31]. The R-spine also contains the HRD-His of the catalytic loop

Table 3
Important residues in selected human protein kinases.

	ALK	EGFR	JAK1	JAK2	MEK1	MEK2	B-Raf
Number of residues	1620	1210	1154	1132	392	400	765
Signal peptide	1–18	1–24	None	None	None	None	None
Extracellular segment	1–1038	25–645	None	None	None	None	None
Transmembrane segment	1039–1061	646–668	None	None	None	None	None
Intracellular portion	1062–1620	669–1210	1–1154	1–1132	1–392	1–400	1–765
Protein kinase domain	1116–1392	712–979	1149–1124	822–1111	68–361	72–367	457–717
Glycine-rich loop	1123–1128	719–724	882–887	856–861	75–80	79–84	464–469
The β3-*K* of *K*/E/D/D	K1150	K745	K908	K882	K97	K101	K483
αC-*E* of K/*E*/D/D	E1167	E762	E925	E898	E114	E118	E501
Gatekeeper residue	L1196	T790	M956	M929	M143	M147	T529
Hinge-residues	1197–1202	791–796	957–962	930–935	144–150	148–154	530–536
Catalytic HR*D* residue, the first *D* of K/E/*D*/D	D1249	D837	D1003	D976	D190	D194	D576
Catalytic loop	1247–1254	835–842	1001–1008	974–981	188–195	192–199	574–58
AS *D*FG, the second *D* of K/E/D/*D*	D1270	D853	D1021	D994	D208	D212	D594
AS threonine/tyrosine phosphorylation site	Y1278	Y869	Y1034/Y1035	Y1007/Y1008	S218/S222	S222/S226	T599/S602
End of the AS	E1299	E884	E1051	E1024	E233	E237	E623
Molecular weight (kDa)	176.4	134.3	133.3	130.7	43.4	44.4	84.4
UniProtKB ID	Q9UM73	P00533	P23458	O60674	Q02750	P36507	P15056

and the DFG-Phe of the activation segment, both within the C-terminal lobe. The HRD-His N–H backbone forms a hydrogen bond with the side chain of a canonical aspartate within the hydrophobic αF-helix. From the bottom to the top, Meharena et al. named the R-spine residues RS0, RS1, RS2, RS3, and RS4 [33]. We later named the C-spine residues from the base to the apex as residues CS1–8 (Fig. 1B/D/F) [34]. We noted that both spines of active protein kinases are linear (Fig. 1B). In enzymes with the DFG-D_{out} conformation, the DFG-D residue (RS2) is displaced leftward and the R-spine is fractured (Fig. 1D). The RS3 is displaced rightward in protein kinases with the αC_{out} conformation (Fig. 1F). The R-spine, C-spine, and shell residues of the five protein kinases considered in this article are provided in Table 4.

The placement of the protein kinase spine and shell residues plays a significant role in establishing the functionality of these enzymes; one cannot overstate their importance in sustaining the activity of this enzyme family as well as the contribution they make in interacting with small molecule protein kinase antagonists. For an outline of the properties of the spine and shell residues and their interactions with small molecule inhibitors of important members of the protein kinase family, see the following articles: Refs. [35–37] for the EGFR family (ErbB1/2/3/4) of protein-tyrosine kinases, Refs. [38–40] for the ALK midkine and pleotrophin receptor protein-tyrosine kinase, Ref. [41] for protein-tyrosine kinases of the fibroblast growth factor receptor family, Ref. [42] for the protein-tyrosine kinases of the PDGFRα/β group, Ref. [43] for the RET glial-cell derived receptor protein-tyrosine kinase, Ref. [44] for the protein-tyrosine kinase corresponding to the Kit stem cell receptor, Ref. [45] for the protein-tyrosine kinase corresponding to the Flt3 receptor, Ref. [46] for the ROS1 orphan receptor protein-tyrosine kinase, Ref. [47] for the protein-tyrosine kinases of the VEGFR1/2/3 family, Refs. [48,49] for the nonreceptor Janus protein-tyrosine kinases, Ref. [50] for the Bruton nonreceptor protein-tyrosine kinase, Refs. [51,52] for the nonreceptor Src protein-tyrosine kinase, Ref. [53] for the nonreceptor BCR-Abl protein tyrosine kinase, Ref. [54] for the dual specificity MEK1/2 protein kinases, Ref. [55] for the CDK4/6 protein-serine/threonine kinases, Refs. [56–58] for the ERK1/2 protein-serine/threonine kinases, Refs. [59,60] for the RAF protein-serine/threonine kinases, and Ref. [9] for phosphatidylinositol 3-kinase (PI3K), a member of the atypical protein kinase group.

The protein kinase catalytic spine consists of two residues from the aminoterminal-lobe and six residues from the carboxyterminal lobe. The ATP adenine connects the two parts of the C-spine and this action facilitates the merging of the two lobes and promotes catalysis [32]. The two amino-terminal lobe residues that bind to the adenine portion of ATP include the conserved β2-strand valine (CS7) following the glycine-rich loop and the conserved β3-strand alanine (CS8) of the AxK signature. A hydrophobic amino acid side chain from the center of the large lobe β7-strand (CS6) interacts with the adenine portion of ATP.

Table 4
Spine and shell residues of selected human kinase domains.

	Symbol	KLIFS No.	ALK	EGFR	JAK1	JAK2	MEK1	MEK2	B-RAF
Regulatory spine									
β4-strand (N-lobe)	RS4	38	C1182	L777	Y940	Y913	F129	F134	F516
C-helix (N-lobe)	RS3	28	I1171	M766	L929	L902	L118	L122	L505
Activation loop DFG-F (C-lobe)	RS2	82	F1271	F856	F1022	F995	F209	F213	F595
Catalytic loop HRD-H (C-lobe)	RS1	68	H1247	H835	H1001	H974	H188	H192	H574
F-helix (C-lobe)	RS0	None	D1311	D896	D1063	D1036	D245	D249	D638
R-Shell									
Two residues upstream from the gatekeeper	Sh3	43	I1194	L788	L954	L927	I141	I145	I527
Gatekeeper, end of β5-strand	Sh2	45	L1196	T790	M956	M929	M143	M148	T529
αC-β4 loop	Sh1	36	V1180	C775	V938	V911	V127	V131	V511
Catalytic Spine									
β2-strand (N-lobe)	CS8	15	A1148	A743	A906	A880	A95	A99	A481
β3-AxK-A (N-lobe)	CS7	11	V1130	V726	V889	V863	V82	V86	V471
β7-strand (C-lobe)	CS6	77	L1256	L844	L1010	L983	L197	L201	F583
β7-strand (C-lobe)	CS5	78	C1255	V845	V1011	V984	V198	V202	L584
β7-strand (C-lobe)	CS4	76	L1257	V843	V1009	I982	I196	I200	I582
D-helix (C-lobe)	CS3	53	L1204	L798	L964	L937	L151	L155	L537
F-helix (C-lobe)	CS2	None	L1318	L907	T1070	V1043	S252	S256	V645
F-helix (C-lobe)	CS1	None	I1322	T903	L1074	L1047	M256	M260	L649

[a]From Refs. [15,21,22], https://klifs.net/, and https://www.uniprot.org/uniprotkb/.

Additionally, the CS4 and CS5 β-7 strand residues interact with CS3 found in the proximal portion of the αD-helix. Moreover, the CS3 residue interacts hydrophobically with (i) its neighboring CS4 and (ii) CS1 within the αF-helix below it. Both the C- and R-spines interact with the hydrophobic αF-helix below them; the αF-helix contains RS0, CS1, and CS2 and this helix serves as a major underpinning that supports and stabilizes the entire protein kinase domain (Fig. 1B). The protein kinase hinge and the following linker residues connect the small and large protein kinase lobes and the 6-amino N–H group of ATP forms a hydrogen bond with the backbone carbonyl group of the initial hinge residue (not shown). Moreover, the adenine *N*1 group of ATP forms a hydrogen bond with the backbone N–H moiety of the third hinge residue (not shown). Nearly all ATP small-molecule steady-state competitive protein kinase antagonists hydrogen bond with backbone hinge residues, usually with the third hinge residue [34].

Using site-directed mutagenesis, Meharena et al. discovered three residues in murine protein kinase A that stabilize and strengthen the regulatory spine, which they identified as Sh1, Sh2, and Sh3 where Sh refers to shell (Fig. 1B/D/F) [33]. Their Sh1 mutant (V104G) possessed 5 % of the activity of the wildtype protein and their Sh2/Sh3 double mutant (M120G/M118G) lacked all catalytic activity. These results indicate that the shell residues sustain PKA activity. We assume that the corresponding residues in other protein kinases perform a similar stabilizing function. The Sh1 residue is found in the segment connecting the αC-helix and the β4-strand, which is called the back loop. The Sh2 residue (the gatekeeper) is located at the end of the β5-strand just before the hinge segment and the Sh3 residue occurs within the β5-strand two residues upstream from the Sh2 residue.

The term gatekeeper refers to the role that this residue plays in controlling access to a hydrophobic compartment bordering the adenine binding pocket [61,62], a residue that interacts with many small molecule protein kinase blockers. Considerable data show that many small molecule ATP-competitive steady-state protein kinase inhibitors contact the R-spine (RS2/3), the C-spine (CS6/7/8), and shell (Sh1 and Sh2) residues. Ung et al. stated that about three-quarters of the protein kinases have a relatively large gatekeeper residue (e.g., Leu, Met, Phe) while about one-quarter have smaller gatekeeper residues (e.g., Thr, Val) [63]. Of importance in long-term drug efficacy, gatekeeper residues of target protein kinases are common sites of drug-resistant mutations [3,64].

3. Overview of selected receptor-mediated signal transduction pathways

3.1. The Ras-Raf-MEK-ERK (MAP kinase) signaling pathway

Protein kinases perform critical roles in nearly every aspect of cell biology [65–67]. They regulate transcription, cellular growth, proliferation, metabolism, migration, the immune response, and nervous system function. Dysregulation of protein kinase activity occurs in many disorders including cancer and inflammatory diseases. Since regulatory protein phosphorylation includes the action of both protein kinases and phosphoprotein phosphatases, phosphorylation-dephosphorylation constitutes an overall reversible process – in contrast to regulatory proteolytic cascades. The MAP kinase signal transduction module is undisputedly the most important oncogenic pathway in human neoplasms [8–11,68–73]. This very conserved pathway transmits signals from extracellular growth factors, cytokines, and regulatory ligands into the intracellular compartment. The MAP kinase cascade is activated by numerous transmembrane receptors. Activated receptor protein-tyrosine kinases such as EGFR become phosphorylated at tyrosine residues and these phosphorylated sites attract many adapter proteins and GEFs (guanine nucleotide exchange factors) such as SOS (from *Drosophila* son of sevenless). The GEFs facilitate the transformation of inactive Ras-GDP to active Ras-GTP within the inner bilayer of the plasma membrane [9]. Of significance, nearly all Ras signaling occurs within the plasma membrane. The *RAS* (Rat sarcoma) gene family is made up of three members: *HRAS* (Harvey rat sarcoma viral oncogene homolog), *KRAS* (Kirsten rat sarcoma viral oncogene homolog), and *NRAS* (neuroblastoma RAS viral (v-ras) oncogene homolog). These proteins switch between active and inactive forms; the transformation of inactive Ras-GDP to active Ras-GTP turns the switch on while intrinsic Ras-GTPase activity stimulated by GAPs (GTPase Activating Proteins) such as NF1 (neurofibromin-1) turns the switch off (Fig. 3).

The molecular weights of H-Ras, K-Ras, and N-Ras are about 21 kDa [9]. In comparison, GEFs and GAPs are large (150–300 kDa) multi-domain proteins capable of a wide variety of interactions with other proteins and regulatory molecules that modulate the concentration of active and inactive Ras. To activate downstream members of the MAP kinase pathway, Ras-GTP mediates the production of active homodimers or heterodimers consisting of A-Raf, B-Raf, or C-Raf by an elaborate process (the Raf acronym corresponds to Rapidly accelerated fibrosarcoma, first described in mice). A/B/C-Raf are protein-serine/threonine kinases that catalyze the phosphorylation and activation of MEK1/2 where MEK corresponds to MAP/ERK Kinase. MEK1/2, in turn, mediate the phosphorylation and activation of ERK1/2 (Extracellular signal-Regulated protein Kinase).

A/B/C-Raf and MEK1/2 have very restricted substrate specificity [74,75]. The only known substrates of the Raf proteins are MEK1/2 and the only known substrates of MEK1/2 are ERK1/2. To further substantiate their restricted substrate specificity, MEK1/2 are unable to mediate the phosphorylation of denatured ERK1/2 nor do they mediate the phosphorylation of peptides with the sequence corresponding to the activation segments of ERK1/2, the physiological substrates. In contrast to A/B/C-Raf and MEK1/2, ERK1/2 have broad substrate specificity and they are able to mediate the phosphorylation of hundreds of different proteins [11]. The Kinase Suppressor of Ras protein kinases (KSR1/2) are evolutionarily close to A/B/C-Raf [4]. KSR1/2 exhibit impaired protein kinase activity – but they are not kinase dead – and they function as scaffolds to assemble Raf, MEK, and ERK to regulate signaling [11]. The effect of KSR1/2 is context-dependent and varies with the level of the various components of the MAP kinase pathway; consequently, KSR1/2 can be stimulatory or inhibitory.

The MAP kinase signaling module consists of a tier of three protein kinases: (i) MAPK kinase kinase (MAP3K), (ii) MAPK kinase (MAP2K), and (iii) and MAPK [54]. Although A/B/C-Raf are at the proximal portion of the MAP kinase cascade, MEKK1/2/3, COT (also known as cancer Osaka thyroid kinase or MAP3K8), and MLK1/2/3/4 are other MAP3Ks that participate in specialized cell type and stimulation specific

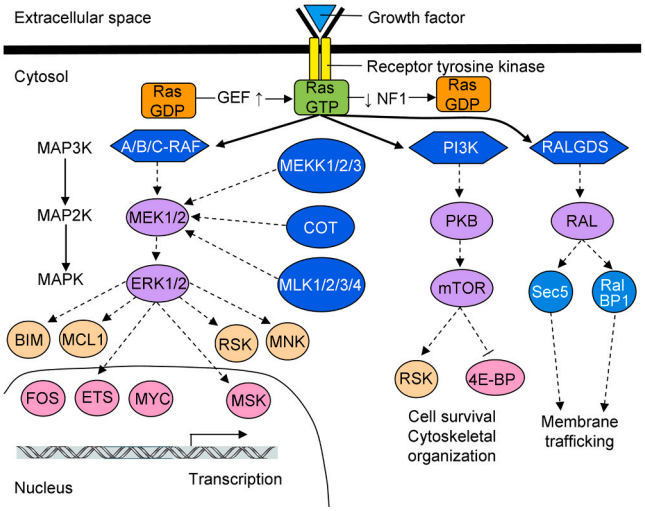

Fig. 3. Overview of the growth factor signal transduction pathway. Adapted from Ref. [57].

responses (Fig. 3) [54]. Ras-GTP has additional downstream effector pathways including the following JAK-STAT (signal transducer and activator of transcription) module.

3.2. JAK/STAT signaling pathways

The JAK (Janus kinase) family of nonreceptor protein-tyrosine kinases consists of four members: JAK1/2/3 and TYK2 (Tyrosine Kinase 2) [76]. These proteins contain an inactive pseudokinase domain (JH2) upstream from an active carboxyterminal protein kinase domain (JH1). The pseudokinase domain decreases the activity of the functional protein kinase domain. Janus is a two-faced Roman God (looking forwards and backwards) whose name was given to this enzyme family owing to the presence of two protein kinase domains within a single polypeptide chain. JAK was whimsically formulated as Just Another Kinase [77]. JAK1/2 and TYK2 are expressed in almost all types of cells while JAK3 is confined to hematopoietic, lymphoid, and myeloid cells [78]. The JAK-STAT pathway conveys extracellular signals from a variety of cytokines, chemokines, growth factors, and hormones to the nucleus [79]. Each of the Janus kinases binds to the intracellular juxtamembrane region of specific cytokine receptors.

The JAK-STAT pathway is responsible for the expression of hundreds of protein-encoding genes (Fig. 4) [79]. Each of the Janus kinases binds to the intracellular juxtamembrane region of specific cytokine or G-protein coupled receptors (GPCR). Numerous actions are necessary for the conversion of an extracellular signal into a transcriptional response. First, cytokine or ligand binding generates conformational changes in their cognate receptor that lead to protein-tyrosine kinase activation resulting from the phosphorylation of two tyrosine residues within the activation segment of the JH1 domain as catalyzed by a partner Janus kinase JH1 enzyme. Following this activation, the JH1 protein kinase domains mediate the phosphorylation of receptor tyrosines that attract the SH2 domain of STATs. The activated JH1 domain then catalyzes the phosphorylation of STAT molecules. These phosphorylated STATS then form dimers that are translocated into the nucleus where they mediate the transcription of target genes. Alternatively, STATs may preexist as dimers and phosphorylation may result in a conformational change that produces activation [80]. Janus kinase activation by EGFR is downstream from the activated receptor and may involve other protein kinases such as Src [79,81].

Humans have seven STAT genes that are identified as *STAT1, STAT2, STAT3, STAT4, STAT5A, STAT5B,* and *STAT6*. Each STAT possesses six

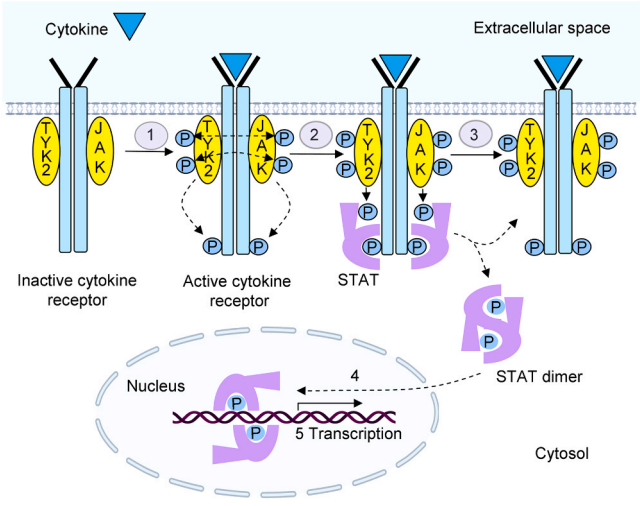

Fig. 4. Overview of the JAK/STAT signaling pathway. The JAK enzymes work in pairs. JAK1 pairs with JAK2/3 and TYK2; JAK2 pairs with JAK1/2 and TYK2 (not JAK3); JAK3 pairs with JAK1 only; TYK2 pairs with JAK1/2. Adapted from Ref. [79].

domains (from the N- to C-terminus) comprising an amino-terminal segment, a coiled-coil domain, a DNA-binding component, a linker fragment, an SH2 domain, and a transcriptional activation domain (TAD), which were first described in STAT1 [82]. TAD contains a tyrosine residue (Y) that is a substrate for an upstream Janus kinase. Following phosphorylation, STATs form homo- or heterodimers that result from the binding of a phosphotyrosine (pY) to the SH2 domain of their partner. The dimer moves into the nucleus where it binds to DNA target sequences alone or in combination with other transcription factors that may enhance or repress DNA transcription.

The STAT family has distinctive roles in signaling. For instance, STAT1 participates in interleukin-9/10 (IL-9/10), thrombopoietin, and interferon signaling while STAT2 is mainly involved in IL-28/29 and interferon-α/β signaling [48,49]. STAT3 takes part in the signaling pathways promoted by many of the Type I, II, and IL-10 families of cytokines. STAT4 participates in the signaling of the Type I heterodimeric cytokines (IL-12/23) and the Type II interferon family cytokines (IL-28/29, IFN-α/β). STAT5A/B take part in the signaling modules initiated by the Type I cytokines with common β-chain or common γ-chain receptor subunits and the hormone-like cytokines. STAT6 participates in IL-3/5 signaling. See Ref. [49] for a general overview of JAK/STAT signaling pathways.

4. A description of protein kinase-inhibitor complexes and inhibitor-binding pockets

Based upon previous publications [62,83–86], we classified small molecule protein kinase inhibitors into seven main groups including reversible (Groups I, I½, II, III, IV, and V) and targeted covalent irreversible inhibitors (VI) as shown in Table 5. We separated type I½ and type II blockers into A and B subtypes [34]. Subtype A agents course past the gatekeeper residue into the back cleft. In contrast, subtype B drugs do not enter the back cleft. The potential importance of this difference, based on preliminary data, is that subtype A antagonists bind to their kinase target with longer residence times when compared with subtype B inhibitors [34]. For instance, sorafenib is a type IIA VEGFR antagonist and sunitinib is a type IIB VEGFR blocker, both of which are FDA-approved for the treatment of renal cell carcinomas. The type IIA antagonist has a residence time greater than 64 min while the type IIB blocker has a residence time of less than 2.9 min [34].

We were guided by the work of Liao, van Linden et al., Kooistra et al., and Kanev et al. [86–89] in analyzing drug-binding pockets. A summary illustrating the location of the binding pockets and subpockets is given in Fig. 5 as expressed in Table 6. The topography between the small and large protein kinase lobes is divided into a front cleft or front pocket, a gate area, and a back cleft. The so-called back pocket (hydrophobic pocket II, or HPII) consists of the gate area and its bordering back cleft. The front cleft includes the glycine-rich loop, the hinge residues, the

Table 5
Classification of small molecule protein kinase inhibitors[a].

Inhibitor type	Properties
I	Binds in and around the ATP-binding pocket of an active enzyme
I½ A/B	Binds in and around the ATP-binding pocket of an inactive DFG-D_{in} enzyme
I½ A	Extends into the back cleft
I½ B	Does not extend into the back cleft
II A/B	Bind in and around the ATP-binding site of an inactive DFG-D_{out} enzyme
II A	Extends into the back cleft
II B	Does not extend into the back cleft
III	Allosteric inhibitor bound next to the ATP-binding site
IV	Allosteric inhibitor bound away from the ATP-binding site
V	Bivalent inhibitor spanning two kinase domain regions
VI	Covalent inhibitor

[a] Ref. [34].

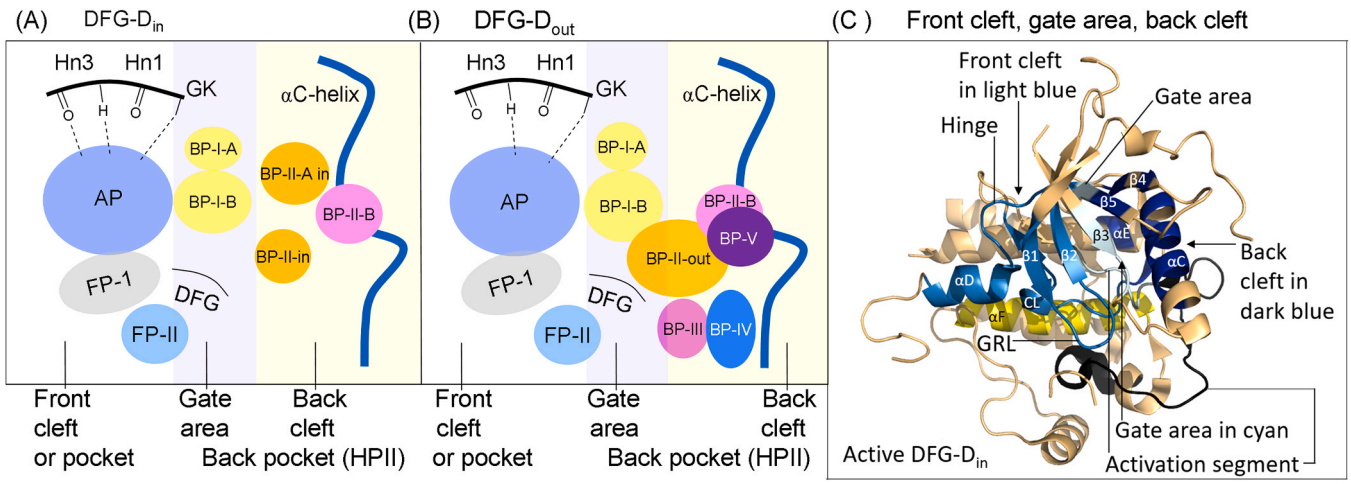

Fig. 5. (A) Location of the protein kinase domain drug-binding pockets in the DFG-D_{in} enzyme form. (B) Location of the drug-binding pockets in the DFG-D_{out} enzyme form. Adapted from Refs. [86–88]. (C) Location of the protein kinase front cleft, gate area, and back cleft. AP, adenine pocket; BP, back pocket; FP, front pocket; Hn, hinge; HPII, hydrophobic pocket II; GK, gatekeeper.

Table 6
Location of important residues within the front cleft, gate area, and back cleft.

Description	Location	KLIFS residue no.[a]
GxGxΦG	Front cleft	4–9
β2-strand V (CS7)	Front cleft	11
β3-strand A (CS8)	Front cleft	15
HRD with DFG-D_{in}	Front cleft	68–70
HRD(x)$_4$N-N	Front cleft	75
β7-strand CS6	Front cleft	77
β3-strand K	Gate area	17
αC-β4 penultimate back loop residue	Gate area	36
Gatekeeper	Gate area	45
The x of xDFG	Gate area	80
DFG	Gate area	81–83
αC-helix E	Back cleft	24
RS3	Back cleft	28
HRD with DFG-D_{out}	Back cleft	68–70

[a] Refs. [88,89].

linker that connects the hinge residues to the αD-helix, the ∝D-helix, the adenine-binding pocket (AP), and the catalytic loop (HRD(x)$_4$N).

Type I antagonists interact with residues in the front cleft [86–89]. The gate area includes residues from both lobes and it contains the last two residues of the β3-strand and the first two residues of the trailing β3-αC loop. It also contains the residue directly before the activation segment (the x of xDFG) along with the first five residues of the activation segment. The back cleft includes the middle residues of the αC-helix and the β4 and β5-strands. The back cleft also includes a portion of the αE-helix as well as the three residues proximal to the catalytic loop HRD. Several type I½ antagonists occur in both the front cleft and a portion of the back cleft. One of the overall goals in the formulation of small molecule protein kinase antagonists is to maximize selectivity and to minimize off-target adverse events [84]; this approach can be enabled by comparing drug interactions with target and nontarget enzymes [90–92]. The formulation of ligand fragments that interact with residues that border the various pockets represents a strategic part of protein kinase inhibitor development with the intention of maximizing drug affinity.

van Linden et al. [87] and Kanev et al. [89] described drug and ligand binding to nearly 6000 human and mouse protein kinases. Their KLIFS (kinase–ligand interaction fingerprint and structure) index includes an arrangement of 85 ligand binding-site residues occurring in both lobes; this information aids in the evaluation of drugs and ligands based upon their binding properties. Such data facilitate the detection of common and unique drug-enzyme interactions. These authors devised a standardized amino acid residue numbering system that assists in the comparison of different protein kinases and their ligands. Table 4 summarizes the relationship of the KLIFS terminology with the C-spine, R-spine, and shell amino acid residue numbering system and Fig. 6 illustrates the location of the KLIFS residues within the protein kinase domain. These authors constructed a valuable noncommercial and searchable web site, which is regularly updated, that provides valuable data on the interaction of protein kinases with ligands and drugs (klifs.net).

Carles et al. posted a comprehensive summary of protein kinase blockers that have been approved by various regulatory agencies or that are in clinical trials [6]. They produced a noncommercial and searchable web site, which is regularly updated, that contains the structures and

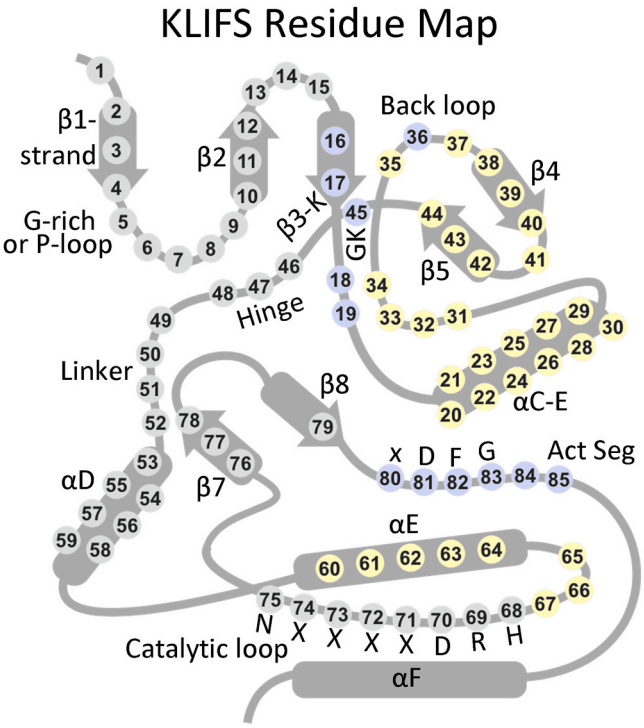

Fig. 6. The location of the KLIFS residues within a generic protein kinase domain. Act Seg, activation segment; GK, gatekeeper. Residues in gray circles are found in the front cleft; blue circles, gate area; yellow circles, back cleft.

physicochemical properties of a variety of medicines, their protein kinase targets, therapeutic indications, trade names, and the year of first approval by regulatory agencies (if applicable) (http://www.icoa.fr/pkidb/). Similarly, the Blue Ridge Institute for Medical Research (BRIMR) provides a web site that lists the FDA-approved protein kinase inhibitors and depicts their (i) molecular structures, (ii) the calculated log of the partition and distribution coefficients, (iii) the number of hydrogen bond donors/acceptors, (iv) the year of initial approval, (v) the number of rings and rotatable bonds, (vi) their primary protein kinase targets, (vii) and their therapeutic indications. This website (www.brimr.org/PKI/PKIs.htm) is regularly updated following the FDA-approval of new protein kinase antagonists.

5. Drug-enzyme interactions: lazertinib, mirdametinib, tovorafenib

5.1. Lazertinib and EGFR

The epidermal growth factor receptor (EGFR) family is one of the most studied receptor protein-tyrosine kinase families because of its general role in signal transduction and in oncogenesis [35,36]. The EGFR family consists of four members that belong to the ErbB lineage of proteins (ErbB1/2/3/4). The ErbB family functions as homo and heterodimers. Seven ligands bind to the extracellular domain and activate EGFR including epidermal growth factor (EGF), transforming growth factor-α (TGFα), amphiregulin (AR), epigen (EPG), betacellulin (BTC), epiregulin (EPR), and heparin-binding epidermal growth-like factor (HB-EGF). Following the binding of the activating ligand to EGFR and the formation of a homodimer or a heterodimer with other members of the EGFR family, the receptor kinase undergoes conformational changes that lead to its phosphorylation and the subsequent activation of downstream signaling pathways that control cell proliferation, motility, invasion, and angiogenesis. Following the extracellular domain is a single transmembrane section consisting of about 25 amino acid residues and an intracellular segment containing about 550 amino acid residues including (i) a small juxtamembrane segment, (ii) a protein kinase catalytic domain, and (iii) a carboxyterminal end. The EGF family of receptors participates in the pathogenesis of a large percentage of lung cancers, which ranks first in the incidence of all types of cancers (excluding skin) worldwide. About 20 % of non-small cell lung cancers possess activating mutations in *EGFR*. Greater than 90 % of these are exon-19 deletions (^{746}ELREA^{750}) or an exon-21 L858R substitution. First generation EGFR antagonists (gefitinib and erlotinib) are orally effective reversible EGFR inhibitors. Regrettably, resistance to these medicines occurs within about one year because of a T790M gatekeeper mutation. Afatinib, dacomitinib, osimertinib, and now lazertinib, which are FDA-approved for the treatment of patients with the exon-19 deletions or the exon-21 substitution mutation, are irreversible inhibitors forming a covalent bond with C797 of EGFR.

Lazertinib is a pyrimidine derivative (Fig. 7A) that forms a covalent bond with *EGFR* (C797) that is approved in combination with amivantamab for the first-line treatment of patients with metastatic NSCLC whose tumors bear *EGFR* exon 19 deletions or the exon 21 L858R substitution mutation [93,94]. Amivantamab is a monoclonal antibody that targets both EGFR and MET (the hepatocyte growth factor receptor protein-tyrosine kinase) and inhibits the binding of their activating ligands and triggers receptor internalization and degradation. The X-ray crystal structure determined by Heppener et al. [95] shows that the *N*1 pyrimidine nitrogen forms a hydrogen bond with the N–H group of M793 – the third hinge residue – and the attached amino group hydrogen bonds with the carbonyl oxygen of M793 (Fig. 8A). Overall, the drug makes hydrophobic contact with two spine residues (CS6/8) and one shell residue (Sh2 – the gatekeeper). The drug also interacts hydrophobically with the β1-strand L718 before the G-rich loop, the β3-strand K745, ^{791}QLMP^{794}, G796, and C797 of the hinge-linker, D800 of the αD-helix, R841 and N842 of the catalytic loop, T845 (the x residue of xDFG), and DFG-D855. Lazertinib binds in the front pocket of an active protein kinase with αC_{in}, DFG-D_{in}, and an open activation segment with an overall active BLAminus conformation [30]; owing to the irreversible nature of the covalent modification of its target enzyme, it is classified as a type VI inhibitor [34]. One advantage of lazertinib is that it is more potent vs. the *EGFR T790M* mutant ($K_i = 2.7$ nM) than the wildtype enzyme ($K_i = 34.6$ nM). This property decreases the likelihood of drug-induced side effects. See Ref. [93] for a review of the studies that led to the approval of this combination therapy for *EGFR* mutation-positive NSCLC.

5.2. Mirdametinib and MEK1

Mirdametinib is an iodoanilino benzamide derivative (Fig. 7B) that inhibits the dual specificity MEK1/2 protein kinases and is FDA-approved for the treatment of neurofibromatosis type-1 (NF1) patients with inoperable plexiform neurofibromas. Neurofibromin is a large molecular weight protein (319 kDa) encoded by the *NF1* gene that

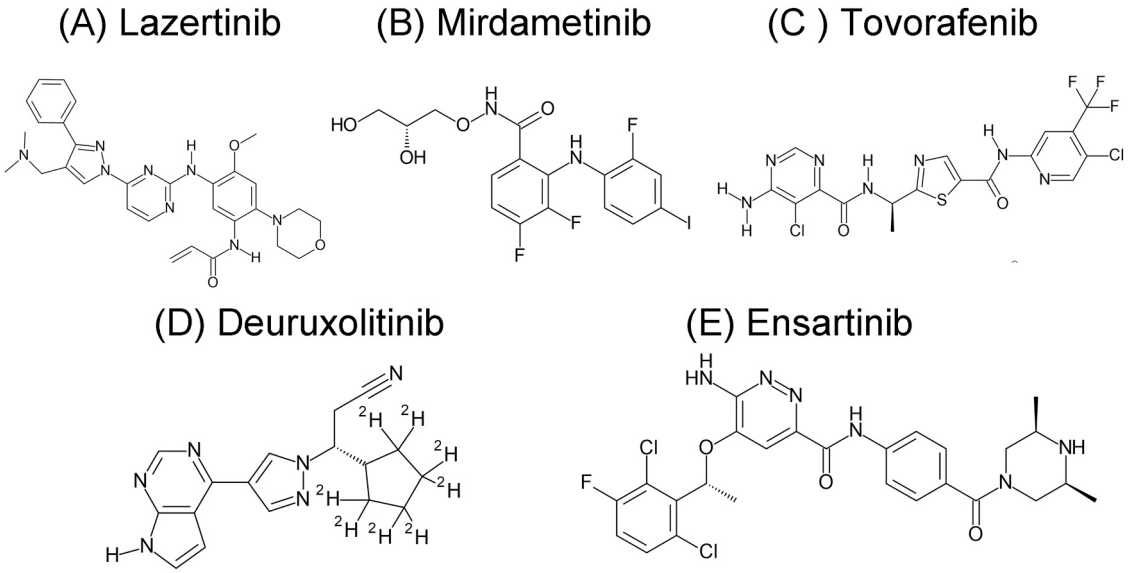

Fig. 7. (A–E). Chemical structures of selected FDA-approved protein kinase antagonists.

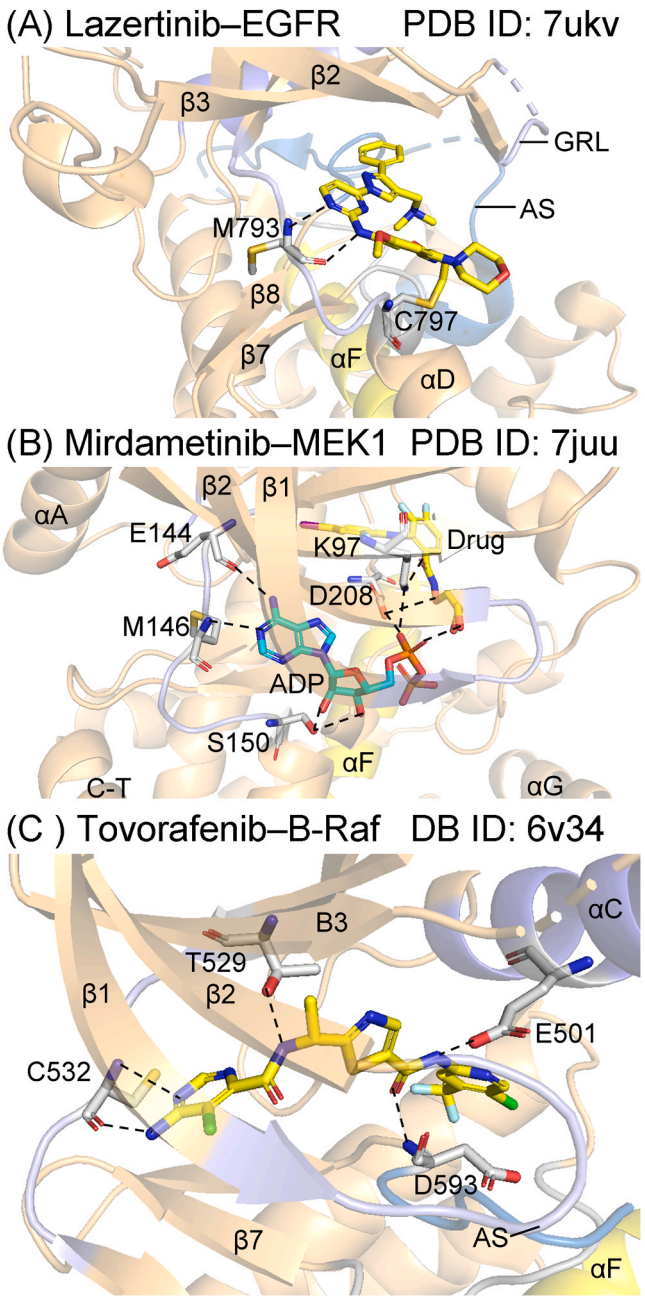

Fig. 8. (A) Lazertinib–EGFR. (B) Mirdametinib–MEK1. (C) Tovorafenib–B-Raf. The respective PDB ID numbers are listed. The drug carbon atoms are colored yellow, the ADP carbon atoms are colored cyan, and the dashed lines represent polar bonds. AS, activation segment; GRL, glycine-rich loop.

stimulates the GTPase activity of Ras [96]. The mutant gene protein is inactive and allows cells to grow in an uncontrolled fashion. As noted above, the MAP kinase signaling pathway participates in the control of numerous cellular processes including cell proliferation, differentiation, and the regulation of apoptosis [54]. MEK1/2 catalyze the phosphorylation of Y204/187 and then T202/185 of ERK1/2 thereby leading to enzyme activation. These residues are found within the ERK1/2 activation segment and the phosphorylation of both residues is necessary for enzyme activation [56,57]. The MAP kinase cascade is perhaps the most important oncogenic driver of human neoplasms and the inhibition of this signaling pathway by targeted antagonists such as mirdametinib is an important antitumor strategy.

Neurofibromatosis-1 is an autosomal dominant genetic disease (1/3000 live births) that usually manifests itself in childhood and the signs and symptoms are usually noticeable shortly after birth [97]. This neurocutaneous disease exhibits tumors in the nervous system and skin. Neurofibromas are benign with miscellaneous cell types including fibroblasts, perineural cells, and Schwann cells. Most affected children exhibit innocuous light-brown café au lait macules that are observed at birth or appear during the first years of life. A finding of more than six café au lait spots strongly suggests a diagnosis of NF1. Additional signs and symptoms of neurofibromatosis type 1 vary, but they can include macrocephaly (an unusually large head), scoliosis (a sideways curvature of the spine), short stature, and hypertension.

Neurofibromas and cafe-au-lait macules are benign and do not require treatment [97]. Symptomatic lesions can be surgically excised, but recurrence is not unusual. Plexiform neurofibromas, which occur in 20–50 % of patients with this disease, involve multiple nerves and are usually present from birth. Plexiform neurofibromas are similar to solitary neurofibromas, but they arise from muscle nerve bundles or fascicles and can infiltrate surrounding structures causing functional impairment and pain. Complete surgical removal is often not possible and the regrowth of the lesion after incomplete surgical resection is common. Plexiform neurofibromas have significant neoplastic potential with an 8–12 % risk to develop into malignant peripheral nerve sheath cancers. Malignant transformation should be considered if (i) the tumor changes from soft-to-hard, (ii) there is a rapid increase in tumor size, (iii) pain ensues for longer than one month, or (iv) new neurologic deficits occur. These neoplasms are treated with wide local excision. Imatinib has been shown to decrease plexiform neurofibroma size, but mirdametinib and selumetinib are preferred options.

Mirdametinib is a selective inhibitor of MEK1/2 with an IC_{50} value of about 0.4 nM (ebi.ac.uk/chembl). Like cobimetinib and selumetinib, mirdametinib is not an ATP steady-state kinetic inhibitor and it binds to MEK1/2 at an allosteric site near the ATP-binding pocket. Fischmann et al. [98] and Khan et al. [99] solved the X-ray crystal structure of mirdametinib and ADP bound to MEK1; that both ADP and the drug can bind simultaneously to the same enzyme conformation indicates that mirdametinib is an allosteric inhibitor. Mirdametinib forms a hydrogen bond with the ε-amino group of AxK-K97, one hydrogen bond with the side chain of DFG-D208, and a third hydrogen bond with the α-phosphate of ADP (Fig. 8B). The compound makes hydrophobic contact with the Sh1 and Sh3 residues (V127, I141). It also makes hydrophobic contact with G79 and G80 of the glycine-rich loop, AxK-K97, L115 of the αC-helix, V127 of the back loop, and ^{209}FGVS^{212}, L215, I216, and M219 of the activation segment. ADP forms hydrogen bonds with the first and third hinge residues (E144, M146) and the ribose moiety forms a hydrogen bond with S150 at the end of the hinge-linker segment. ADP makes hydrophobic contact with three spine residues (CS6/7/8), one shell residue (Sh2), and the KLIFS-3 residue. It also interacts hydrophobically with ^{74}LGAG^{77} within the glycine-rich loop, AxK-K97 and E144, M146 and S150 within the hinge-linker segment, and D152 and Q153 within the αD-helix. Furthermore, it makes hydrophobic contact with K192, S194, and N195 within the catalytic loop and L197 within the β7-strand. Mirdametinib is bound to an inactive enzyme form with a closed activation segment with DFG-D_{in} and αC_{out} and a BLBplus conformation [30]. The drug occurs adjacent to the ATP-binding pocket and is classified as a type III allosteric inhibitor [34]. Type IV allosteric inhibitors bind far from the ATP-binding site.

5.3. *Tovorafenib and B-Raf*

Tovorafenib is a 1,3-thiazocarboxamide derivative (Fig. 7C) that is FDA approved for the treatment of pediatric low grade gliomas in patients harboring a B-Raf–fusion protein or a *BRAF* V600 mutation [100,101]. Most of these tumors show MAPK pathway activation owing to B-Raf dysregulation, which produces aberrant intracellular signaling. Tovorafenib is an inhibitor of mutant *BRAF* V600E (K_i of 20.5 nM), wild-type BRAF (K_i of 6.1 nM), and *BRAF* fusion proteins. Tovorafenib efficacy was evaluated in the FIREFLY-1 (NCT04775485) clinical trial,

which was a single-arm, open-label, multicenter study that enrolled patients six months to 25 years of age with relapsed or refractory low grade glioma with an activating *BRAF* alteration. Pediatric low grade gliomas are the most common CNS tumor diagnosis in children with 1200–1500 new cases in the United States per year. Such tumors have an overall 10-year survival rate of 94 %. However, the 10-year progression-free survival rate for those needing systemic treatment with standard of care chemotherapy (vincristine/carboplatin or vinblastine) is only 44 %. This disorder is considered to be a chronic disease in patients whose tumors are unresectable or cannot be completely resected and such patients often require several treatments throughout life. Late adverse effects include the impairment of neurologic, endocrine, and cognitive functioning. For a summary of the clinical trial that led to the approval of tovorafenib, see Ref. [102].

Tkacik et al. determined the X-ray crystal structure of tovorafenib bound to wildtype and V600E mutant *BRAF* [103]. They observed that the pyrimidine forms a hydrogen bond with the N–H group of C532 and the pyrimidine 6-amino moiety hydrogen bonds with the C532 carbonyl group (Fig. 8 C). The drug also hydrogen bonds with the side chain hydroxyl group of T529 (the gatekeeper residue), the side chain of αC-E501, and the N–H group of DFG-D593. The drug makes hydrophobic contact with three spine residues (RS1, CS7/8) and two shell residues (Sh2/3). Tovorafenib makes hydrophobic contact with the β1-strand I463, and V482 and K483 of the β3-strand, V504 and L505 of the αC-helix, I513 and L514 of the back loop, ^{530}QWC^{532} of the hinge, L567 of the αD-helix, I592 of the β8-strand, xDFG-xG593, and DFG-F595. Modi and Dunbrack found that this enzyme occurs within the inactive BBAminus enzyme cluster with the DFG-D_{out} conformation, which they label as a type II inhibitor [30]. The drug is found in the front pocket, gate area, back pocket, and BP-I-A, BP-I-B and we classify this compound as a type IIA inhibitor because it has the DFG-D_{out} conformation and extends into the back pocket [34].

6. Small molecule FDA-approved kinase antagonists lacking a drug-enzyme structure

6.1. Properties of deuruxolitinib

Deuruxolitinib is a pyrrolo[2,3-*d*]pyrimidine derivative (Fig. 7D) that inhibits the JAK family and is FDA-approved for the treatment of severe alopecia areata in adults (www.brimr.org/PKI/PKIs.htm). Deuruxolitinib is a deuterated form of ruxolitinib, which selectively inhibits JAK1/2 with K_i values of about 0.7 nM (ebi.ac.uk/chembl). Deuteration allows the drug to circumvent extensive oxidative metabolism around the cyclopentyl ring and avoid intestinal breakdown, which increase its duration of action. Alopecia areata is an autoimmune disease that leads to random hair loss in the scalp and other regions of the body [104–108]. The JAK-STAT pathway, which regulates the expression of numerous inflammatory mediators, is linked to the pathophysiology of this disorder. The newly approved deuruxolitinib inhibits the inflammatory actions promoted by the JAK-STAT pathway.

Alopecia areata is exemplified by recurring bouts of hair loss and hair regrowth and is challenging to manage [106]. It can be aggravated by stress and anxiety with an undesirable influence on the quality of life. Patients with alopecia areata have patches of scalp hair loss, while people with more severe disease exhibit complete loss of hair on the scalp (alopecia totalis) or the entire body (alopecia universalis) [109]. Topical corticosteroids and sensitizers were the primary treatments available for mild disease, while oral corticosteroids (methylprednisone), azathioprine or methotrexate (both antimetabolites) were recommended for patients with severe disease [107]. These treatments are of low efficacy and better treatment modalities were needed, prompting the development of JAK inhibitors such as deuruxolitinib and ritlecitinib.

The FDA label carries numerous black box warnings against various infections (bacterial, fungal, opportunistic, viral), pulmonary embolism, sudden cardiovascular death, and malignancies including lung cancer and lymphomas. Moreover, deuruxolitinib is not recommended for use in combination with cyclosporine, biologic immunomodulators, other JAK inhibitors, or other potent immunosuppressants. As noted previously, the JAK family kinases activate STATs. The JAK/STAT pathway upregulates interleukin-15 (IL-15) and interferon-γ, which activate $CD8^+$ T cells. The $CD8^+$ T cells target hair follicle cells and this process is implicated in the pathogenesis of alopecia areata [106]. The deuruxolitinib blockade of JAK family kinases expressed in hematopoietic cells further decreases the immune attack on the hair follicles and blunts the inflammatory response. The drug demonstrated good clinical efficacy and a favorable safety profile despite the black box warnings. See Refs. [104,105,108] for a summary of the clinical trials that led to the FDA-approval of deuruxolitinib.

6.2. Properties of ensartinib

Ensartinib is an aminopyridazine derivative (Fig. 7E) that is FDA-approved for the first-line treatment of advanced ALK-positive NSCLC (www.brimr.org/PKI/PKIs.htm). It is a potent inhibitor of wildtype ALK with an IC_{50} of less than 4 nM [110]. It also inhibits ALK F1174, C1156Y, L1196M, S1206T, and T1151 mutants with similar IC_{50} values. Ensartinib also antagonizes the activity of TPM3-TRKA, TRCK, GOCP-ROS, EphA1, EphA2, and MET with values in the low nM range. Siegel et al. estimated that about 226,000 new cases of lung cancer will be diagnosed in the United States in 2025 (110,000 men and 116,000 women) and 124,000 people will die of the disease (64,000 men and 60,000 women) [111]. Lung cancer deaths account for about one-fifth of all cancer-related deaths in the United States and about 18 % worldwide. The median age at the time of diagnosis of lung cancer in the United States is at 71 years [112]. About 80 % of lung malignancies are non-small cell lung cancers (NSCLC); the remainder are small cell lung cancers and various other tumor types.

The EML4 (echinoderm microtubule-associated protein-like 4)-ALK fusion protein and seven additional ALK-fusion proteins (KLC1, HIP1, KIF5B, TFG, STRN, PTPN3, TPR) play an essential role in the development of about 5 % of non-small cell lung cancers [112]. Physiological ALK is a receptor protein-tyrosine kinase that participates in nervous system development and is related to the insulin receptor; the nature of the ALK ligand is unclear. The amino-terminal portions of the ALK fusion proteins result in dimerization and subsequent activation of the ALK protein kinase domain that plays a key role in the pathogenesis of various tumors. Downstream signaling from the ALK fusion protein leads to the activation of the MAP kinase cell proliferation module and the JAK/STAT pathways.

Crizotinib was the first inhibitor approved by the FDA for the treatment of ALK-positive NSCLC in 2011 [39,113]. The median time for the development of crizotinib drug resistance was about 10.5 months following the initiation of therapy. Such resistance motivated the development of second- and third-generation drugs including alectinib, brigatinib, ceritinib and lorlatinib, which are approved for the treatment of ALK-positive NSCLC. Unlike the single gatekeeper mutation that occurs in drug-resistant EGFR in lung cancer, about a dozen different mutations in the catalytic domain of ALK fusion proteins have been described that produce crizotinib resistance. Ensartinib demonstrated good clinical activity in patients with prior crizotinib treatment, in patients that were ALK kinase inhibitor naïve, and in patients with CNS lesions at the time of diagnosis; the medicine was generally well tolerated. See Refs. [114–116] that describes the clinical trials that led to the approval of ensartinib.

7. Physicochemical properties of orally bioactive drugs

7.1. Lipinski's rule of five (Ro5)

Medicinal chemists and pharmacologists have examined the

physicochemical properties of drugs that are orally effective to learn how to formulate new orally bioavailable medicinals [117]. Lipinski's rule of five (Ro5) is a computational and experimental technique that is used to predict membrane permeability and efficacy in the drug-discovery venue [118]. It is a guideline that evaluates drug-likeness and ascertains whether a compound with specific pharmacological activities has properties indicating that it would be orally active. The Lipinski benchmarks were founded on information indicating that most orally effective medicines are comparatively small and moderately lipophilic in nature. The Ro5 is used during drug development as pharmacologically active lead compounds are serially optimized to increase their activity while maintaining selectivity.

The Ro5 criteria suggest that less than ideal oral efficacy is more likely to result when (i) the AlogP (atom-based calculated Log P) is greater than 5, when (ii) there are more than 5 hydrogen-bond donors, when (iii) there are more than 5 × 2 or 10 hydrogen-bond acceptors, and when (iv) the molecular weight is greater than 5 × 100 or 500 [118]. The partition coefficient (P) is the ratio of the concentration of the un-ionized drug in the organic phase divided by its concentration in the aqueous phase of water-saturated *n*-octanol. The P value signifies the hydrophobicity of a compound; the larger the P value, the greater the hydrophobicity. The number of hydrogen-bond donors is the sum of the number of OH and NH groups. The number of hydrogen-bond acceptors represents the number of nitrogen and oxygen atoms attached to at least one hydrogen atom in its neutral state.

The Ro5 criteria were based on the physicochemical properties of more than two thousand orally effective drugs [118]. Excluding the macrolides (everolimus, sirolimus, and temsirolimus), the average molecular weight (MW) of the FDA-approved protein kinase antagonists is 472 ranging from 285 (ritlecitinib) to 615 (trametinib) (Table 7). The drugs with a molecular weight exceeding 500 include the three macrolides and 28 other antagonists including the newly approved lazertinib and tovorafenib. Although these data indicate that there is a tendency for orally effective small molecule protein kinase blockers to exceed the 500 Da molecular-weight criterion, the masses of most of the larger compounds excepting the macrolides are close to 500 Da. Moreover, a total of 24 of the 85 approved drugs have an ALogP of greater than 5.0. Additionally, dabrafenib, fostamatinib, tovorafenib, and the three macrolides have more than ten hydrogen bond acceptors (Table 7).

In summary, a total of 39 of the 85 FDA-approved small molecule protein kinase antagonists fail to satisfy Lipinski's Ro5. Of these 39, the following have two Ro5 exceptions (a molecular weight greater than 500 and a partition coefficient greater than 5) including bosutinib, brigatinib, cabozantinib, entrectinib, infigratinib, lapatinib, midostaurin, mobocertinib, neratinib, nilotinib, and ripretinib. Dabrafenib, everolimus, and serolimus have three Ro5 deficiencies with a molecular weight greater than 500, more than 10 hydrogen bond acceptors, and an ALogP greater than 5. These are FDA-approved medicines, but finding drug candidates during the discovery process with two or three Ro5 criteria exceptions is normally an unwanted result.

7.2. The importance of lipophilicity and ligand efficiency

7.2.1. Lipophilic efficiency, LipE

Following the appearance of Lipinski's Ro5 in 2001 [118], subsequent studies of the chemical and physical properties of orally bioavailable medicines have led to numerous refinements [119–126]. For instance, lipophilic efficiency, or LipE, is a property that is employed in drug development that amalgamates potency and lipophilic-facilitated binding as a strategy to increase drug efficacy. The following equations define lipophilic efficiency:

$$\text{LipE} = \text{p}IC_{50} - \text{ALogP};\ \text{LipE} = \text{p}K_i - \text{ALogP}$$

Like the practice of designating the molar hydrogen ion concentration as pH, the operator p denotes the negative of the Log of the K_i or IC_{50}. Furthermore, ALogP is the atom-based calculated Log of the Partition coefficient; this parameter depicts the ratio of drug content in the organic phase divided by its concentration in the aqueous phase of immiscible *n*-octanol/water.

The second expression in the equation (– ALogP or minus ALogP) signifies the lipophilicity of a drug and the value is calculated using an algorithm based upon the properties of thousands of prototypical organic compounds. The greater the concentration of a medicine in the organic phase when compared with the aqueous phase of a *n*-octanol/water mixture, the greater is its lipophilicity. Leeson and Springthorpe stated that drug lipophilicity, as assessed by its – ALogP value, is a crucial property that should be measured during drug discovery [120]. Their use of – ALogP was founded on observations made before the calculation of the distribution coefficient (D) became standard. The distribution coefficient ($LogD_{7.4}$) is the ratio of the content of the ionized and un-ionized substance in the organic phase over the aqueous phase of immiscible *n*-octanol/water at a specified pH of the aqueous phase, which is usually set at 7.4. In practice, either $LogD_{7.4}$ or ALogP can be employed to monitor several compounds in the same investigation. Note that large negative ALogP values in the defining formula reduce the lipophilic efficiency.

An elevated lipophilicity may lead to the binding of a medication to adventitious targets and such binding may increase toxicity. A common objective during drug development and discovery is to increase potency without simultaneously increasing lipophilicity. The use of lipophilic efficiency aids in the betterment of lead compounds by comparing a series of drug congeners; furthermore, an identical methodology for determining the lipophilic efficiency should be used to make certain that such comparisons are valid [122,123]. To cite a relevant example, Cui et al. described the optimization of lead compounds during the fabrication of crizotinib using lipophilic efficiency as a marker of binding effectiveness [113]; crizotinib is approved by the FDA for the treatment of ROS1-positive and ALK-positive NSCLC.

The ALogP of various drug candidates can be computed in seconds to minutes. Because experimental determinations of LogP are labor intensive, such measurements are not routinely performed. Hopkins et al. noted that satisfactory values for LogP are less than ~ 3 and reasonable values of lipophilic efficiency are greater than ~ 5 [122]. Increasing potency and decreasing lipophilicity throughout drug discovery normally produces products with improved pharmacological properties. The average value of lipophilic efficiency (LipE) for 82 FDA-approved small molecule protein kinase antagonists (omitting the three macrolides) is 4.56 with a range from 1.3 (neratinib) to 7.96 (deucravacitinib) (Table 8). The average value for ALogP for the 82 FDA-approved drugs (excluding the three macrolides) was 3.96 with a range from 1.1 (baricitinib) to 6.36 (ceritinib and nilotinib).

7.2.2. Ligand efficiency, LE

The ligand efficiency (LE) relates binding affinity, or potency, to the number (N) of heavy (nonhydrogen) atoms in a drug. The following formula is used to calculate this property:

$$\text{LE} = \Delta G^{\circ\prime}/\text{N} = -\text{RT ln } K_{eq}/\text{N} = -2.303\text{RT Log } K_{eq}/\text{N}$$

$\Delta G^{\circ\prime}$ is the standard free energy change of an agent binding to its target enzyme at neutral pH, R denotes the energy-temperature coefficient or universal gas constant (1.98×10^{-3} kcal/degree-mol), T is the temperature in degrees Kelvin, K_{eq} is the value of the equilibrium constant, and N represents the number of nonhydrogen or heavy atoms in the drug. The IC_{50} or K_i values are surrogates for the equilibrium constant. At a physiological temperature of 37°C (310 K), this equation becomes $-(2.303 \times (1.98 \times 10^{-3}/\text{K}) \times 310\text{ K Log } K_{eq})/\text{N}$ or $-1.41 \text{ Log } K_{eq}/\text{N}$. Some investigators use a temperature of 300 K and the multiplication factor becomes – 1.37 [122,126]. Ligand efficiency is an indication of ligand potency based upon the average binding energy per nonhydrogen atom. Ligand efficiency is useful in fragment-based drug

Table 7
Properties of FDA-approved small molecule inhibitors.

Drug	PubMED CID	MW (Da)	HD[a]	HA[b]	ALogP[c]	Log $D_{7.4}$[d]	PSA (Å^2)[e]	nStereo[f]	Cplx[g]
Abemaciclib	46220502	507	1	9	4.94	3.76	75	0	723
Abrocitinib	78323835	323	2	6	1.3	0.79	99.4	0	474
Acalabrutinib	71226662	466	2	6	3.31	2.56	119	1	845
Afatinib	10184653	486	2	8	4.39	2.34	88.6	1	702
Alectinib	49806720	483	1	5	4.77	4.75	72.4	0	867
Asciminib	72165228	450	3	8	3.46	3.86	103	1	626
Avapritinib	118023034	499	1	9	2.61	2.12	106	1	752
Axitinib	6450551	386	2	4	4.64	4.15	96	0	557
Baricitinib	44205240	371	1	7	1.10	−0.19	129	0	678
Belumosudil	11950170	452	3	6	4.82	4.65	105	0	678
Binimetinib	10288191	441	3	7	3.01	3.81	88.4	0	521
Bosutinib	5328940	530	1	8	5.19	3.37	82.9	0	734
Brigatinib	68165256	584	2	9	5.09	2.49	85.9	0	835
Cabozantinib	25102847	501	2	7	5.54	4.65	98.8	0	795
Capivasertib	25227436	429	4	6	2.10	–0.16	120	0	580
Capmatinib	25145656	412	1	6	3.43	2.96	85.1	0	637
Ceritinib	57379345	558	3	8	6.36	3.38	114	0	835
Cobimetinib	16222096	531	3	7	3.78	2.73	64.6	1	624
Crizotinib	11626560	450	2	6	5.04	0.95	78	1	558
Dabrafenib	44462760	520	2	11	5.36	5.10	147	0	817
Dacomitinib	11511120	470	2	7	5.16	3.53	79.4	0	665
Dasatinib	3062316	488	3	9	3.31	3.74	135	0	642
Deucravacitinib	134821691	426	3	8	1.73	2.10	136	0	648
Deuruxolitinib	72704611	314	1	4	3.47	2.48	83.2	1	453
Encorafenib	50922675	540	3	10	3.91	2.61	149	1	836
Ensartinib	56960363	561	3	8	4.73	3.26	122	3	812
Entrectinib	25141092	561	3	8	5.03	4.87	85.5	0	847
Erdafitinib	67462786	446	1	7	4.18	1.25	77.3	0	583
Erlotinib	176870	393	1	7	3.41	3.20	74.7	0	525
Everolimus	6442177	958	3	14	6.20	7.40	205	15	1810
Fedratinib	16722836	525	3	9	4.82	3.23	117	0	787
Fostamatinib	11671467	580	4	15	3.09	−0.52	187	0	904
Fruquintinib	44480399	393	1	7	3.85	2.64	95.7	0	579
Futibatinib	71621331	418	1	7	1.78	1.77	108	1	723
Gefitinib	123631	447	1	8	4.28	3.64	68.7	0	545
Gilteritinib	49803313	552	3	10	2.70	1.69	121	0	785
Ibrutinib	24821094	441	1	6	4.22	3.63	99.2	1	678
Imatinib	5291	494	2	7	4.59	3.80	86.3	0	706
Infigratinib	53235510	560	2	8	5.35	3.99	95.1	0	724
Lapatinib	208908	580	2	9	6.14	4.40	115	0	898
Larotrectinib	46188928	428	2	7	2.95	2.44	86	2	659
Lazertinib	121269225	555	2	9	4.10	3.56	110	10	837
Lenvatinib	9823820	427	3	5	4.07	2.52	116	0	634
Lorlatinib	71731823	406	1	7	2.80	1.62	110	1	700
Midostaurin	9829523	571	1	4	5.91	5.43	77.7	4	1140
Mirdametinib	9826528	482	4	8	2.47	3.98	90.8	7	465
Mobocertinib	118607832	586	2	9	5.08	3.79	114	0	935
Momelotinib	25062766	414	2	7	2.98	2.70	103	0	615
Neratinib	9915743	557	2	8	5.93	3.05	112	0	881
Netarsudil	66599893	454	2	5	4.89	3.42	94.3	1	678
Nilotinib	644241	530	2	9	6.36	5.35	97.6	0	817
Nintedanib	135423438	540	2	7	3.62	2.57	101	0	892
Osimertinib	71496458	500	2	7	4.51	3.01	87.6	0	752
Pacritinib	46216796	473	1	7	4.47	1.96	67.7	0	644
Palbociclib	5330286	448	2	8	2.97	1.30	103	0	775
Pazopanib	10113978	438	2	8	3.14	3.55	127	0	717
Pemigatinib	86705695	487	1	8	3.66	1.80	83.2	0	731
Pexidartinib	25151352	417	2	7	5.23	4.45	66.5	0	537
Pirtobrutinib	129269915	479	3	9	3.43	3.35	125	1	719
Ponatinib	24826799	533	1	8	4.46	4.54	65.8	0	910
Pralsetinib	129073603	534	3	9	4.20	3.64	136	1	816
Quizartinib	24889392	561	2	9	5.86	5.05	106	0	849
Regorafenib	11167602	483	3	8	5.69	4.49	92.4	0	686
Repotrectinib	135565923	355	2	6	2.55	2.17	80.6	0	524
Ribociclib	44631912	435	2	7	2.80	0.91	91.2	0	636
Ripretinib	71584930	510	3	5	5.67	4.38	86.4	0	746
Ritlecitinib	118115473	285	2	4	1.94	1.40	73.9	2	402
Ruxolitinib	25126798	306	1	4	3.47	2.48	83.2	1	453
Selpercatinib	134436906	526	1	9	3.28	3.11	112	0	885
Selumetinib	10127622	458	3	6	3.53	4.27	88.4	0	523
Sirolimus	5284616	914	3	13	6.18	7.45	195	15	1760
Sorafenib	216239	465	3	7	5.55	4.34	92.4	0	646
Sunitinib	5329102	398	3	4	3.33	1.28	77.2	0	636
Temsirolimus	6918289	1030	4	16	4.39	?	242	15	2010

(*continued on next page*)

Table 7 (*continued*)

Drug	PubMED CID	MW (Da)	HD[a]	HA[b]	ALogP[c]	Log $D_{7.4}$[d]	PSA (Å^2)[e]	nStereo[f]	Cplx[g]
Tepotinib	25171648	493	0	7	4.01	2.26	94.7	0	880
Tivozanib	9911830	455	2	7	5.64	4.16	108	0	631
Tofacitinib	9926791	312	1	5	1.54	1.19	88.9	2	488
Tovorafenib	25161177	506	3	11	3.98	2.99	164	5	695
Trametinib	11707110	615	2	6	3.94	3.18	102	0	1090
Trilaciclib	68029832	447	2	7	2.72	2.29	91.2	0	707
Tucatinib	51039094	481	2	8	5.09	5.25	111	0	796
Upadacitinib	58557659	380	2	6	2.91	0.85	78.3	2	561
Vandetanib	3081361	475	1	7	4.43	2.14	59.5	0	539
Vemurafenib	42611257	490	2	7	5.54	4.61	100	0	790
Zanubrutinib	135565884	472	2	5	4.22	3.42	103	0	756

[a] HD, no. of hydrogen bond donors.
[b] HA, no. of hydrogen bond acceptors.
[c] ALogP, values for atom-based log of the partition coefficient from https://www.ebi.ac.uk/chembl/.
[d] Log $D_{7.4}$, values for the log of the distribution coefficients at pH 7.4 obtained from https://www.ebi.ac.uk/chembl/.
[e] PSA, polar surface area values obtained from https://pubchem.ncbi.nlm.nih.gov/.
[f] Defined atom stereocenter count.
[g] Complexity values obtained from https://pubchem.ncbi.nlm.nih.gov/.

discovery procedures and, like lipophilic efficiency, it aids in the formulation and selection of congeners of lead compounds for additional development [123].

Ligand efficiency reflects the binding affinity per heavy atom of the drug or ligand of interest. The value of N is a proxy for the molecular weight. The equation used to compute ligand efficiency demonstrates that its value is directly proportional to the binding affinity or – Log K_{eq} (a positive number) and is inversely proportional to the number of heavy atoms. Hopkins et al. noted that satisfactory values for ligand efficiency (LE) are greater than 0.3 kcal per mole per heavy atom [119,122]. Ligand efficiency values for the FDA-approved small molecule protein kinase blockers based upon representative K_i or IC_{50} values are included in Table 8. The average value for ligand efficiency for 82 of the FDA-approved protein kinase inhibitors (excluding the three macrolides) was 0.369 with a range from 0.237 (mobocertinib) to 0.631 (ritlecitinib). Nine drugs had values of less than 0.3 including mobocertinib, midostaurin, neratinib, nintedanib, nilotinib, fostamatinib, pacritinib, and the newly approved lazertinib and tovorafenib. The values for lipophilic efficiency (LipE) and ligand efficiency (LE) listed in Table 8 are based on data acquired using different experimental protocols. Consequently, these assessments cannot be used to make direct comparisons of the drugs because different methodologies were employed to obtain the data. These results were obtained from diverse drug development studies and thus provide representative values.

7.2.3. Additional chemical descriptors of orally effective drugs

To determine drug properties related to oral efficacy, the Ro5 has prompted the development of many variations. For instance, Veber et al. reported that the number of rotatable bonds and the polar surface area (PSA) differs between orally active and inactive compounds in a large series of drugs in rats [124]. They found that an optimal number of rotatable bonds is 10 or fewer. This characteristic modulates passive membrane permeation and signifies molecular flexibility or degrees of freedom. Moreover, molecular flexibility is linked to the entropy change that transpires from ligand binding and governs the quantity of drug bound to its targets. With the eception of five drugs with 11 rotatable bonds (erlotinib, fedratinib, lapatinib, neratinib, temsirolimus) and mobocertinib with 13 rotatable bonds, the remaining 79 drugs have 10 or fewer of these bonds (Table 8). The average value is 6.34 and the number of rotatable bonds ranges from 0 (repotrectinib, lorlatinib) to 13 (mobocertinib). Moreover, Veber et al. found that most orally bioavailable medicines have a polar surface area less than or equal to 140 Å^2 [124]. This parameter represents the sum of the surface over all polar atoms, primarily oxygen and nitrogen, and it also includes any connected hydrogen atoms. Excluding the three macrolides, the average value for the surface area is 99.4 Å^2 with a range from 59.5 (vandetanib) to 187 (fostamatinib). Dabrafenib, encorafenib, fostamatinib, and the newly approved tovorafenib are the only drugs with a polar surface area exceeding 140 Å^2 (Table 7). Moreover, Oprea remarked that the number of ring structures (both aromatic and nonaromatic) in most approved bioavailable drugs is three or more [125]. All FDA approved small molecule protein kinase antagonists have three or more rings (except the newly approved mirdametinib) with an average value of 4.24 and a range from two (mirdametinib) to seven (midostaurin) (Table 8). Except for netarsudil (an eye drop) and trilaciclib and temsirolimus (which are given intravenously), all of the FDA-approved drugs are orally effective. Additionally, ruxolitinib is employed orally and topically.

The molecular complexity of a medicine is based upon its structure, the elements it contains, and its symmetry. The complexity is computed using the Bertz/Hendrickson/Ihlenfelt procedure [127,128]. It is based upon the number of its constituent atoms, the bonding arrangement, and the nature of the chemical bonds (single, double, triple, aromatic). Molecular complexity ranges from 0 for ions to several thousand for intricate natural products. Larger chemicals generally exhibit a greater molecular complexity than smaller substances. In contrast, compounds that are highly symmetrical and containing few elements are characterized by smaller molecular complexity values. The complexity values for the FDA-approved agents in this article were obtained from PubChem (https://pubchem.ncbi.nlm.nih.gov/). For the 85 FDA-approved kinase inhibitors, the average complexity value is 707 with a range from 402 (ritlecitinib) to 2010 (temsirolimus) (Table 7). As anticipated, the three higher molecular weight macrolide compounds have the greatest molecular complexity values. There are no optimal or recommended molecular complexity values for orally effective medicines; however, this property can be helpful in predicting the ease or difficulty of drug synthesis, a significant consideration in the manufacture of commercial pharmaceuticals. Analogously, the occurrence of numerous stereocenters in medicines may make drug synthesis more problematic.

Leeson et al. compared drug properties in two periods: 1990–2009 and 2010–2020 [126]. They reported that the molecular weight and lipophilicity of approved drugs increased with time. We compared the averages of selected properties of FDA-approved protein kinase antagonists during the periods from 2001 – 2017 and 2018 – 2025, periods which gave about an equal number of drugs. This analysis excluded the three macrolides. We observed an increase in the average molecular weight (463–480 Da), lipophilic efficiency (4.29–4.84), and ligand efficiency (0.356–0.441). However, the average number of hydrogen bond donors and acceptors, ALopP, polar surface area, molecular complexity, number of rotatable bonds, ring count, and potency (K_i value) were similar (Tables 7 and 8). Leeson et al. found that the molecular weight of all FDA-approved drugs, including protein kinase antagonists, increased over their time frame [126].

Table 8
Properties of FDA-approved small molecule protein kinases inhibitors.

Drug	Target, kinase family[a]	K_i nM[b]	pK_i	LipE[c]	N*[d]	LE[e]	Dose[f]	Sol[g]	nRotB[h]	nRng[i]	nAr[j]	nBnz[k]	QED[l]
Abemaciclib	CDK4, S/T	0.6	9.22	4.28	37	0.351	400*	15.9	7	5	4	0	0.38
Abrocitinib	JAK1, NRY	5.1	8.29	7.04	22	0.531	100	420	6	3	2	0	0.83
Acalbrutinib	BTK, NRY	3.1	8.51	5.20	35	0.343	200*	10.9	4	5	4	1	0.45
Afatinib	EGFR, RY	0.5	9.33	4.94	34	0.387	40	12.8	8	4	3	1	0.46
Alectinib	ALK, RY	1.9	8.72	3.95	36	0.342	1200*	10.5	3	6	3	0	0.58
Asciminib	BCR-Abl, NRY	0.5	9.3	5.84	31	0.300	80	55	6	4	3	1	0.50
Avapritinib	PDGFRα, RY	0.18	9.7	7.09	37	0.370	300	30.1	5	6	5	1	0.39
Axitinib	VEGFR2, RY	0.25	9.6	4.96	28	0.483	300	0.55	5	4	4	1	0.52
Baricitinib	JAK2, NRY	7	8.15	7.05	26	0.442	2	357	5	4	3	0	0.72
Belumosudil	ROCK2, S/T	53.9	7.3	2.48	34	0.303	200	2.89	7	5	5	1	0.33
Binimetinib	MEK1, DS	12	7.92	4.91	27	0.414	90*	49.9	6	3	3	1	0.40
Bosutinib	BCR-Abl, NRY	20	7.7	2.51	36	0.302	500	9.5	9	4	3	1	0.38
Brigatinib	ALK, RY	0.398	9.4	4.31	40	0.331	180	22	8	5	3	2	0.35
Cabozantinib	RET, RY	5	8.3	2.76	37	0.316	40	1.99	8	5	4	2	0.31
Capivasertib	AKT=PKB, S/T	3	8.52	6.42	30	0.400	800	> 1000	6	4	3	1	0.48
Capmatinib	MET, RY	0.13	9.89	6.46	31	0.450	800*	5.29	4	5	5	1	0.49
Ceritinib	ALK, RY	0.2	9.7	3.34	38	0.360	750	2.22	9	4	3	2	0.28
Cobimetinib	MEK1, DS	0.79	9.1	5.32	30	0.428	60	42.2	4	4	2	2	0.53
Crizotinib	ALK, RY	0.63	9.2	4.16	30	0.432	500*	6.11	5	4	3	1	0.53
Dabrafenib	B-Raf, S/T	0.4	9.4	4.04	35	0.379	300*	3.27	6	4	4	2	0.37
Dacomitinib	EGFR, RY	2	8.7	3.54	33	0.372	45	8.74	7	4	3	1	0.47
Dasatinib	BCR-Abl, NRY	0.16	9.8	6.49	33	0.419	100	12.8	7	4	3	1	0.47
Deucravacitinib	TYK2, NRY	0.2	9.69	7.96	31	0.441	6	0.159	7	4	3	1	0.52
Deuruxolitinib	JAK2/1, NRY	0.7	9.15	5.68	23	0.561	16*	120	4	4	3	0	0.80
Encorafenib	B-Raf, S/T	0.3	9.52	5.61	36	0.373	450	11.2	10	3	3	1	0.37
Ensartinib	ALK, RY	0.4	9.4	4.68	38	0.349	225	6.4	6	4	3	2	0.37
Entrectinib	TRKA, RY	1	9	3.97	41	0.310	600	8.9	7	6	4	2	0.29
Erdafitinib	FGFR1, RY	2	8.7	4.52	33	0.372	8	13	9	4	4	1	0.41
Erlotinib	EGFR, RY	0.32	9.5	6.09	29	0.462	150	8.91	11	3	3	1	0.42
Everolimus	FKBP12/mTOR, S/T	?	?	?	68	?	10	1.63	9	3	0	0	0.13
Fedratinib	JAK2, NRY	6	8.22	3.40	37	0.313	400	9.49	11	4	3	2	0.35
Fostamatinib	Syk, RY	17	7.77	4.68	40	0.274	300*	52	10	4	3	1	0.26
Fruquintinib	VEGFR2, RY	35	7.46	3.61	29	0.363	5	0.0803	5	4	4	0	0.55
Futibatinib	FGFR2, RY	4	8.4	6.62	31	0.382	20	40	6	4	3	1	0.51
Gefitinib	EGFR, RY	0.5	9.3	5.02	31	0.423	250	27	8	4	3	1	0.52
Gilteritinib	Flt3, RY	0.41	9.39	6.69	40	0.331	120	22.3	9	5	2	1	0.43
Ibrutinib	BTK, NRY	12.6	7.9	3.68	33	0.338	560	20.3	5	5	4	2	0.47
Imatinib	BCR-Abl, NRY	1	9	4.41	37	0.343	600	14.6	7	5	4	2	0.39
Infigratinib	FGFRs, RY	5	8.3	2.95	38	0.308	125	29.9	8	4	3	2	0.38
Lapatinib	EGFR, RY	1	9	2.86	40	0.317	1250	22.3	11	5	5	2	0.18
Larotrectinib	TRK, RY	9.7	8.01	5.06	31	0.364	200*	238	3	5	3	1	0.67
Lazertinib	EGFR, RY	10.2	7.99	3.88	41	2.75	240	25	10	5	4	2	0.28
Lenvatinib	VEGFR2, RY	3.98	8.4	4.33	30	0.395	24	6.22	6	4	3	1	0.55
Lorlatinib	ALK, RY	9	8.05	5.25	30	0.378	100	108	0	3	3	1	0.61
Midostaurin	Flt3, RY	37	7.43	1.52	43	0.244	200*	15.7	3	7	4	1	0.29
Mirdametinib	MEK1/2, Y/T	0.4	9.4	6.76	26	0.510	2	31.3	7	2	2	2	0.36
Mobocertinib	EGFR, RY	60	7.22	2.14	43	0.237	160	13.6	12	4	4	1	0.17
Momelotinib	JAK2/1, NRY	1.4	8.85	5.87	31	0.402	200	32.5	6	4	3	2	0.60
Neratinib	ErbB2/HER2, RY	59	7.23	1.30	40	0.255	240	6.74	11	4	4	1	0.22
Netarsudil	ROCK1/2, S/T	1	9	4.11	34	0.373	0.01	0.23	8	4	4	2	0.39
Nilotinib	BCR-Abl, NRY	12.5	7.9	1.54	39	0.286	600*	2.01	6	5	5	2	0.27
Nintedanib	FGFR, RY	39.8	7.4	3.78	40	0.261	300*	30.9	8	5	4	2	0.35
Osimertinib	EGFR, RY	7	8.15	3.64	37	0.311	80	22.4	10	4	4	1	0.31
Pacritinib	JAK2, NRY	19	7.72	2.21	35	0.289	100	38	4	4	2	1	0.67
Palbociclib	CDK4, S/T	10	8	5.03	33	0.342	125	17.4	5	5	3	0	0.58
Pazopanib	VEGFR2, RY	30	7.52	4.38	31	0.342	800	43.3	5	4	4	1	0.49
Pemigatinib	FGFR, RY	0.5	9.3	5.64	35	0.375	13.5	144	6	5	3	1	0.57
Pexidartinib	CSF1R, RY	13	7.89	2.66	29	0.384	800*	3.15	5	4	4	0	0.47
Pirtobrutinib	BTK, NRY	0.5	9.3	5.87	34	0.386	200	3.84	7	3	3	2	0.45
Ponatinib	BCR-Abl, NRY	1	9	4.54	39	0.325	45	2.95	6	5	4	2	0.39
Pralsetinib	RET, RY	0.5	9.3	5.10	39	0.336	400	10.1	8	5	4	0	0.31
Quizartinib	Flt3, RY	3.3	8.48	2.62	40	0.299	35.4	50.9	8	5	3	1	0.26
Regorafenib	VEGFR2, RY	4.2	8.4	2.71	33	0.359	160	1.02	5	3	3	2	0.41
Repotrectinib	ROS1, RY	0.07	11.2	8.60	26	0.607	320*	49.8	0	3	3	1	0.65
Ribociclib	CDK4, S/T	10	8	5.20	32	0.353	600	231	5	5	3	0	0.64
Ripretinib	RET, RY	3	8.52	2.85	33	0.364	150	5.83	5	4	4	2	0.32
Ritlecitinib	JAK3, NRY	33.1	7.48	5.54	21	0.502	50	457	3	3	2	0	0.85
Ruxolitinib	JAK1, NRY	1.2	8.92	5.45	23	0.547	20*	116	4	4	3	0	0.8
Selpercatinib	RET, RY	1	9	5.72	39	0.325	320*	29.9	8	4	4	0	0.37
Selumetinib	MEK1, DS	14	7.85	4.32	27	0.410	80*	21	6	3	3	1	0.39
Sirolimus	FKBP12/mTOR, S/T	?	?	?	65	?	2	1.73	6	3	0	0	0.16
Sorafenib	VEGFR1, RY	15.8	7.8	2.25	32	0.344	800*	1.71	5	3	3	2	0.46
Sunitinib	VEGFR2, RY	3.98	8.4	5.07	29	0.408	50	30.8	7	3	2	0	0.63
Temsirolimus	FKBP12/mTOR, S/T	?	?	?	73	?	25**	2.35	11	4	0	0	?

(*continued on next page*)

Table 8 (*continued*)

Drug	Target, kinase family[a]	K_i nM[b]	pK_i	LipE[c]	N*[d]	LE[e]	Dose[f]	Sol[g]	nRotB[h]	nRng[i]	nAr[j]	nBnz[k]	QED[l]
Tepotinib	MET, RY	1	9	4.99	37	0.343	450	?	7	5	4	2	0.38
Tivozanib	VEGFR2, RY	6.5	8.19	2.55	32	0.312	1.34	52.1	6	4	4	1	0.39
Tofacitinib	JAK1, NRY	0.79	9.1	7.56	23	0.558	10*	299	3	3	2	0	0.93
Tovorafenib	B-Raf, S/T	10	8	4.02	32	0.285	600**	1.94	5	3	3	0	0.48
Trametinib	MEK1, DS	3.4	8.47	4.53	37	0.323	2	30.7	5	5	3	2	0.33
Trilaciclib	CDK4/6, S/T	1	9	6.28	33	0.385	480	260	3	6	3	0	0.64
Tucatinib	ErbB2/HER2, RY	8	8.1	3.01	36	0.317	600*	4	6	6	5	1	0.36
Upadacitinib	JAK1, NRY	43	7.37	4.46	27	0.385	15	70.7	3	4	3	0	0.73
Vandetanib	RET, RY	50	7.3	2.30	30	0.343	300	10.2	6	4	3	1	0.59
Vemurafenib	B-Raf, S/T	3.98	8.4	2.86	33	0.359	1920*	0.36	7	4	4	2	0.33
Zanubrutinib	BTK, NRY	0.3	9.52	5.30	35	0.384	320*	10.3	6	5	3	2	0.52

[a] NRY, non-receptor protein-tyrosine kinase; RY, receptor protein-tyrosine kinase; S/T, protein-serine/threonine kinase; DS; dual specificity protein kinase (catalyzes protein-tyrosine and then threonine phosphorylation of target kinase activation segments but evolutionarily in the protein-serine/threonine kinase family).
[b] Representative values obtained from www.ebi.ac.ug/chembl/ and from klifs.net.
[c] LipE (lipophilic efficiency) = $p\mathrm{IC}_{50}$ – ALogP
[d] N*, Number of heavy (nonhydrogen) atoms.
[e] LE (ligand efficiency) = – 2.303 RT Log_{10} K_i/N where N is the number of heavy (non-hydrogen) atoms in the drug
[f] Dosage in mg/day from FDA label; *, one-half of total daily dose taken twice per day; **, once weekly.
[g] Sol, solubility (μg/ml) in water (go.drugbank.com/drugs/)
[h] nRotB, number of Rotatable Bond values obtained from https://pubchem.ncbi.nlm.nih.gov/.
[i] nRng, number of rings
[j] nAr, number of Aromatic rings
[k] nBnz, number of benzene moieties
[l] QED, summed, weighted desirability (scores using MW + ALogP + HBD + HBA + PSA + nRotB + nAr) obtained from https://www.ebi.ac.uk/chembl/; see Ref. [126] for a full explanation.

Ritchie and Macdonald examined the role of aromaticity on the pharmacological properties of various medicines within the perspective of drug design and discovery [129]. Aromaticity is related to cyclically conjugated organic chemicals with a stability that is substantially greater than that of a localized Kekulé structure owing to electron delocalization. They counted aromatic bicyclic and tricyclic compounds as structures that contain two and three aromatic rings, respectively. Aromatic rings include structures containing carbon alone or with nitrogen or sulfur heteroatoms. These investigators found that increasing the number of carboaromatic rings had an unfavorable effect on pharmacologic properties by decreasing aqueous solubility, increasing binding to serum albumin, and inhibiting cytochrome P450. We find that the mean number of aromatic rings in the 85-approved protein kinase antagonists was 3.2 and the average number of benzene moieties was 1.07 (Table 8). All the FDA-approved kinase antagonists, excepting the three macrolides, have a minimum of two aromatic rings and a maximum of five. Eighteen of the drugs lacked benzene moieties and the number of drugs possessing one or two benzenes was about evenly distributed among the remainder (Table 8).

Bayliss et al. evaluated the dose and water solubility for orally effective drug and drug candidates [130]. They reported that daily doses of 100 mg or less reduced the risk of toxicity. The range of dosages for protein kinase blockers given orally is from 1.34 mg to 1920 mg daily with an average of about 280 mg (Table 8). The daily doses range from 1.34, 2.0, and 2.0 mg for tivozanib, trametinib, and baricitinib and 1200, 1250, and 1920 mg for alectinib, lapatinib, and vemurafenib, respectively. Only 35 of the 85 FDA-approved kinase antagonists are prescribed with daily dosages of 100 mg or less. Bayliss et al. reported that medicines with a water solubility of 100 μg/ml or less are associated with an increased risk of failure during drug development and clinical trials [130]. We examined the solubility of the FDA-approved protein kinase blockers in water and found a range from 0.08 μg/ml (fruquintinib) to 457 μg/ml for the ritlecitinib with a mean value of about 50 μg/ml. This calculation excludes tepotinib and capivasertib; there is no information in the public domain on the solubility of tepotinib and the latter is freely soluble in water. Only 12 of the 85 drugs including capivasertib have a solubility greater than 100 μg/ml. The dosages and solubilities among the FDA-approved kinase blockers spread over three orders of magnitude.

8. Epilogue and perspective

Although investigators have made significant progress in the development and discovery of orally effective small molecule protein kinase inhibitors since the FDA-approval of imatinib in 2001, this field is still in its early stages. Oprea et al. proposed that the altered activity of many understudied protein kinases potentially plays a critical role in the pathogenesis of tumors [131]. Furthermore, such understudied kinases are potential drug targets. Examples include cyclin-dependent protein kinase 12 (CDK12), mitogen-activated protein kinase kinase kinase 1 (MAP3K1), ribosomal protein S6 kinase δ1 (RPS6KC1), and eukaryotic elongation factor 2 kinase (EEF2K). Most of the FDA-approved protein kinase inhibitors are antineoplastic while the remainder function as immunomodulators [10,132–135]. Because of the ingrained genetic changes in benign and malignant cancers, resistance to protein kinase antagonists occurs on a nearly universal basis. Such resistance motivated the production of second, third, and later generation inhibitors that target (i) the initial enzyme and (ii) activators of bypass pathways. Gatekeeper mutations in the initial protein kinase target are often the cause of acquired drug resistance [3]. For example, a gatekeeper mutation in *EGFR* (T790M) is a representative case in lung cancers. Significantly, this substitution accounts for about half of all acquired *EGFR* inhibitor resistance mutations.

Because 244 protein kinase genes map to cancer amplicons or disease loci [8], we expect that (i) there will be a significant increase in the number of drugs blocking more protein kinases and (ii) new drugs will be developed for the treatment of many more illnesses [136–139]. Adding additional protein kinase targets to the therapeutic arsenal will require the elucidation of signaling pathways besides the MAP kinase and phosphatidylinositol 3-kinase/AKT/mTOR signaling modules [140]. Besides the 85 approved protein kinase blockers considered in this review, the FDA has approved five orally bioavailable drugs that inhibit phosphatidylinositol 3-kinases (PI3Ks are members of the atypical protein kinase family) [9]. These PI3K blockers include alpelisib – a PI3K-α inhibitor that is used for the treatment of breast cancer – and duvelisib, copanlisib, umbralisib and idelalisib, which are PI3K-δ inhibitors that are prescribed for the third-line management of follicular lymphomas and other hematological disorders. As the protein kinase inhibitor field develops, it is probable that protein kinase antagonists

with new chemotypes, pharmacophores, and scaffolds will be engineered [141]. We anticipate that additional allosteric inhibitors will be developed that inhibit enzymes besides MEK1/2 that are part of various protein kinase signal transduction modules [142,143]. Moreover, it is probable that additional irreversible inhibitors that target protein kinases with –SH groups near the ATP-binding site will become available. There is also a major effort in combining protein kinase inhibitor therapy with various immunomodulators for the management of lung, renal, and breast, carcinomas [112,144,145].

Of the 85 FDA-approved drugs, receptor protein-tyrosine kinases are the chief targets of 46 of them followed by nonreceptor protein-tyrosine kinases (21), protein-serine/threonine kinases (13), and dual-specificity protein kinases (5) (Table 1). Members of the EGFR/ErbB family represent the top-ranked target (11) followed by the JAK, VEGFR, BCR-Abl, ALK, and the FGFR family. CDK4/6 is inhibited by four of the FDA-approved drugs that are used for the treatment of breast cancer. The dual specificity (MEK1/2) protein kinases, which inhibit the RAS-Raf-MEK MAP kinase module, include cobimetinib (used in combination with vemurafenib for the treatment of melanoma), binimetinib (used in combination with encorafenib for the management of melanoma), trametinib (used in combination with dabrafenib for the treatment of melanoma, NSCLC with *BRAF* V600E/K mutations, and advanced thyroid cancer), and selumetinib and the newly approved mirdametinib (prescribed for the management of neurofibromatosis I).

The clinical effectiveness of medicines that are FDA-approved for the management of chronic myelogenous leukemia (CML) is much greater than other protein kinase inhibitors that are used for the treatment of other diseases. Patients with CML treated with BCR-Abl antagonists have an annual mortality rate of 0.5 % or less when compared with age-matched control groups [146,147]. This indicates that BCR-Abl blockers normalize the life span of CML patients. Imatinib (first generation), nilotinib, dasatinib, and bosutinib (second generation) are approved by the FDA for first-line therapy while ponatinib and asciminib (third generation) are prescribed for patients with resistant disease and a T315I mutation or after failure with at least two other protein-tyrosine kinase blockers [148]. Asciminib is a STAMP (Specifically Targeting the Abl Myristoyl Pocket) type IV allosteric antagonist prescribed for the first-line treatment of CML patients with the *T315I* mutation and as a third-line CML treatment [135].

The goal in the management of CML is to promote patient survival and to attain treatment-free remission (TFR) whenever possible [53]. For promoting survival, frontline treatment with imatinib, nilotinib, dasatinib, or bosutinib are all successful [149]. If imatinib is prescribed for the first-line treatment, a modification in treatment at the first indication of resistant disease is currently the standard practice. One reason for prescribing imatinib at the outset is its availability as a generic drug with a lower cost than that of the other medicines. The choice of the second-line treatment is guided by a determination of potential mutations of the Abl kinase domain and by the patient's age and co-morbidities [147]. Side effects produced by nilotinib include pancreatitis (1 %–3 %), the exacerbation of diabetes mellitus (5 %–10 %), and hyperglycemia (10 %–15 %). Adverse events produced by dasatinib include pulmonary hypertension (1 %–2 %), pleural effusions (10 %–15 %), and myelosuppression (10 %–20 %). Bosutinib can produce diarrhea (10 %–30 %, which is mild and self-limited) and liver and kidney dysfunction. Ponatinib leads to the most serious adverse events including pancreatitis (5 %), skin rashes (5 %–10 %), vasospastic disease (10 %–15 %), and hypertension (20 %–30 %) [147].

Attaining treatment-free (TFR) remission is appropriate in younger people to avoid lifelong drug therapy. A deep molecular response (DMR), which is a 0.01 % reduction in the BCR-Abl-1 transcripts on the International Scale (the ratio of BCR-Abl1 transcripts to Abl1 transcripts), is one benchmark for terminating drug therapy. Discontinuing drug treatment after a deep molecular response lasting (i) two or three years is linked to a treatment-free remission rate of 50 %–60 % and lasting (ii) five years is coupled with a treatment-free remission rate of about 80 %. When treatment-free remission is not achieved, patients fortunately respond to the treatment used before drug withdrawal. For further discussion of approaches for achieving treatment-free remission, see Refs. [147,149–151]. The concept of treatment-free remission for CML was inconceivable at the beginning of the targeted protein kinase treatment era. In the early 21st century, the notion that drug treatment for CML could be discontinued and the disease would remain in check was a fantasy.

Dasatinib was one of the early drugs used in the treatment of CML following its approval in 2006. It was discovered via the use of high throughput screening (HTS) initiated by the Pfizer pharmaceutical company in 1986 [152]. HTS involves the use of 96-well plates with assay volumes of 50–100 μL. By 1992 HTS produced successful starting materials for about 40 % of the drug discovery portfolio. By 1999 ADMET (Absorption, Distribution, Metabolism, Excretion, and Toxicity) HTS was completely integrated into the drug discovery process. At this time the Ro5 methodology was instituted to maximize the discovery of effective drugs and to minimize the attrition of drug leads that were identified by HTS. Gefitinib, erlotinib, sorafenib, and lapatinib are additional early FDA-approved protein kinase blockers that resulted from HTS hits. Before the advent of high throughput screening, drug discovery was based upon experiments performed in live animals. The formal definitions of drug and drug-likeness can be nebulous as exemplified by the following – in the 1970s I learned from Professor John P Long, a classical pharmacologist at the University of Iowa that "A drug is a substance, that when injected into an animal, produces a paper."

The generally used drug descriptors and properties used by pharmacologists and medicinal chemists are listed in Table 9. Beyond Ro5 (bRo5) descriptors include the molecular weight, $LogD_{7.4}$, polar surface area, number of rings, number of stereocenters, number of rotatable bonds, potency, ligand efficiency metrics, and composite metrics such as quantitative estimate of drug likeness (QED) [126,153]. Poor passive cell permeability, low solubility, and concerns related to metabolism are correlated with increased lipophilicity and molecular weight. These problems must be overcome when working in the bRo5 space. Increased molecular complexity frequently increases solubility and decreases adventitious binding to off-targets. The protein kinase inhibitor field is relatively new and 39 of the 85 FDA-approved drugs (46 %) have a least one Ro5 violation. As stated by Hartung et al. "Playing by the rules is thus not always advisable when pushing for success in drug discovery. Rather, successful drug hunters must follow a mindset of pushing the limits of what is possible. Now, 25 years after the publication of the Ro5, small-molecule drug discovery is looking at an exciting future of clinical impact that must not be restricted by the number 5" [154].

Table 9
Drug properties and descriptors[a].

Category	Properties and descriptions
Size	Molecular weight (MW) and heavy atom count (N)
Lipophilicity	Calculated octanol–water partition coefficients (ALogP and Log $D_{74.}$
Polarity	Polar surface area (PSA), hydrogen-bond donors (HD) and hydrogen-bond acceptors (HA)
Aromatic and aliphatic descriptors	Number of rings (nRng), number of aromatic rings (nAr), number of benzene rings (nBnz), fraction of carbon atoms that are sp^3 hybridized (Fsp3), number of stereocenters (nStereo)
Flexibility	Number of rotatable bonds (nRotB)
Potency	$-Log_{10}$ molar concentration IC_{50} or K_i as pIC_{50} or pK_i
Ligand efficiency metrics	Lipophilic ligand efficiency or LipE = pIC_{50} – AlogP or pIC_{50} – Log $D_{7.4;}$ Ligand efficiency or LE = pIC_{50} /N
Composite physicochemical descriptors	Quantitative estimate of drug-likeness or QED = summed, weighted desirability (scores using MW + ALogP + HD + HA + PSA + nRotB + nAr)

[a] Adapted from Ref. [126].

CRediT authorship contribution statement

Robert Roskoski: Writing – review & editing, Writing – original draft, Project administration, Methodology, Conceptualization.

Declaration of Competing Interest

The author is unaware of any affiliations, memberships, or financial holdings that might be perceived as affecting the objectivity of this review.

Acknowledgements

I thank Dr. Albert J. Kooistra for providing the template depicted in Fig. 6 and Laura M. Roskoski for providing editorial and bibliographic assistance. I also thank Jasper Martinsek and Josie Rudnicki for their help in preparing the figures and W.S. Sheppard and Pasha Brezina for their help in the analyses of drug properties. The colored figures in this paper were evaluated to ensure that their perception was accurately conveyed to colorblind readers [155].

Appendix A. Supporting information

Supplementary data associated with this article can be found in the online version at doi:10.1016/j.phrs.2025.107723.

Data Availability

No data was used for the research described in the article.

References

[1] P. Cohen, Protein kinases – the major drug targets of the twenty-first century? Nat. Rev. Drug Discov. 1 (2002) 309–315, https://doi.org/10.1038/nrd773.
[2] R. Roskoski Jr., A historical overview of protein kinases and their targeted small molecule inhibitors, Pharm. Res. 100 (2015) 1–23, https://doi.org/10.1016/j.phrs.2015.07.010.
[3] P. Cohen, D. Cross, P.A. Jänne, Kinase drug discovery 20 years after imatinib: progress and future directions, Nat. Rev. Drug Discov. 20 (2021) 551–569, https://doi.org/10.1038/s41573-021-00195-4.
[4] M.M. Attwood, D. Fabbro, A.V. Sokolov, S. Knapp, H.B. Schiöth, Trends in kinase drug discovery: targets, indications and inhibitor design, Nat. Rev. Drug Discov. 20 (2021) 839–861, https://doi.org/10.1038/s41573-021-00252-y. Author correction. Nat Rev Drug Discov 2021;20:798. doi: 10.1038/s41573-021-00303-4.
[5] G.K. Kanev, C. de Graaf, I.J.P. de Esch, R. Leurs, T. Würdinger, B.A. Westerman, A.J. Kooistra, The landscape of atypical and eukaryotic protein kinases, Trends Pharm. Sci. 40 (2019) 818–832, https://doi.org/10.1016/j.tips.2019.09.002.
[6] F. Carles, S. Bourg, C. Meyer, P. Bonnet, PKIDB: a curated, annotated and updated database of protein kinase inhibitors in clinical trials, pii: E908, Molecules 23 (2018), https://doi.org/10.3390/molecules23040908.
[7] J.J. Adashek, M. Nikanjam, R. Kurzrock, Tumour-agnostic kinase inhibitors, Nat. Rev. Drug Discov. (2025), https://doi.org/10.1038/s41573-025-01147-y.
[8] G. Manning, D.B. Whyte, R. Martinez, T. Hunter, S. Sudarsanam, The protein kinase complement of the human genome, Science 298 (2002) 1912–1934, https://doi.org/10.1126/science.1075762.
[9] R. Roskoski Jr., Properties of FDA-approved small molecule phosphatidylinositol 3-kinase inhibitors prescribed for the treatment of malignancies, Pharm. Res. 168 (2021) 105579, https://doi.org/10.1016/j.phrs.2021.105579.
[10] R. Roskoski Jr., Properties of FDA-approved small molecule protein kinase inhibitors, Pharm. Res. 144 (2019) 19–50, https://doi.org/10.1016/j.phrs.2019.03.006.
[11] R. Roskoski Jr., Properties of FDA-approved small molecule protein kinase inhibitors: a 2020 update, Pharm. Res. 152 (2020) 104609, https://doi.org/10.1016/j.phrs.2019.104609.
[12] R. Roskoski Jr., Properties of FDA-approved small molecule protein kinase inhibitors: a 2021 update, Pharm. Res. 165 (2021) 105463, https://doi.org/10.1016/j.phrs.2021.105463.
[13] R. Roskoski Jr., Properties of FDA-approved small molecule protein kinase inhibitors: a 2022 update, Pharm. Res. 175 (2022) 106037, https://doi.org/10.1016/j.phrs.2021.106037.
[14] R. Roskoski Jr., Properties of FDA-approved small molecule protein kinase inhibitors: a 2023 update, Pharmacol Res 2023, Pharm. Res. 187 (2023) 106552, https://doi.org/10.1016/j.phrs.2022.106552.
[15] R. Roskoski Jr., Properties of FDA-approved small molecule protein kinase inhibitors: a 2024 update, Pharm. Res. 200 (2024) 107059, https://doi.org/10.1016/j.phrs.2024.107059.
[16] S.H. Myers, V.G. Brunton, A. Unciti-Broceta, AXL inhibitors in cancer: a medicinal chemistry perspective, J. Med Chem. 59 (2016) 3593–3608, https://doi.org/10.1021/acs.jmedchem.5b01273.
[17] B.L. Roth, D.J. Sheffler, W.K. Kroeze, Magic shotguns versus magic bullets: selectively non-selective drugs for mood disorders and schizophrenia, Nat. Rev. Drug Discov. 3 (2004) 353–359, https://doi.org/10.1038/nrd1346.
[18] R. Roskoski Jr., Orally effective FDA-approved protein kinase targeted covalent inhibitors (TCIs), Pharm. Res. 165 (2021) 105422, https://doi.org/10.1016/j.phrs.2021.105422.
[19] R. Roskoski Jr., Futibatinib (Lytgobi) for cholangiocarcinoma, Trends Pharm. Sci. 44 (2023) 190–191, https://doi.org/10.1016/j.tips.2022.12.007.
[20] D.R. Knighton, J.H. Zheng, L.F. Ten Eyck, V.A. Ashford, N.H. Xuong, S.S. Taylor, J.M. Sowadski, Crystal structure of the catalytic subunit of cyclic adenosine monophosphate-dependent protein kinase, Science 253 (1991) 407–414, https://doi.org/10.1126/science.1862342.
[21] A.P. Kornev, S.S. Taylor, Dynamics-driven allostery in protein kinases, Trends Biochem. Sci. 40 (2015) 628–647, https://doi.org/10.1016/j.tibs.2015.09.002.
[22] R. Roskoski Jr., Cyclin-dependent protein serine/threonine kinase inhibitors as anticancer drugs, Pharm. Res. 139 (2019) 471–488, https://doi.org/10.1016/j.phrs.2018.11.035.
[23] R. Roskoski Jr., Hydrophobic and polar interactions of FDA-approved small molecule protein kinase inhibitors with their target enzymes, Pharm. Res. 169 (2021) 105660, https://doi.org/10.1016/j.phrs.2021.105660.
[24] S.K. Hanks, T. Hunter, Protein kinases 6. The eukaryotic protein kinase superfamily: kinase (catalytic) domain structure and classification, FASEB J. 9 (1995) 576–596.
[25] Madhusudan, E.A. Trafny, N.H. Xuong, J.A. Adams, L.F. Ten Eyck, S.S. Taylor, J. M. Sowadski, cAMP-dependent protein kinase: crystallographic insights into substrate recognition and phosphotransfer, Protein Sci. 3 (1994) 176–187, https://doi.org/10.1002/pro.5560030203.
[26] J. Zhou, J.A. Adams, Participation of ADP dissociation in the rate-determining step in cAMP-dependent protein kinase, Biochemistry 36 (1997) 15733–15738, https://doi.org/10.1021/bi971438n.
[27] P.A. Schwartz, B.W. Murray, Protein kinase biochemistry and drug discovery, Bioorg. Chem. 39 (2011) 192–210, https://doi.org/10.1016/j.bioorg.2011.07.004.
[28] A.P. Kornev, S.S. Taylor, Defining the conserved internal architecture of a protein kinase, Biochim Biophys. Acta 1804 (2010) 440–444, https://doi.org/10.1016/j.bbapap.2009.10.017.
[29] V. Modi, R.L. Dunbrack Jr., Defining a new nomenclature for the structures of active and inactive kinases, Proc. Natl. Acad. Sci. USA 116 (2019) 6818–6827, https://doi.org/10.1073/pnas.1814279116.
[30] V. Modi, R.L. Dunbrack Jr., Kincore: a web resource for structural classification of protein kinases and their inhibitors, Nucleic Acids Res. 50 (2022) D654–D664, https://doi.org/10.1093/nar/gkab920.
[31] A.P. Kornev, N.M. Haste, S.S. Taylor, L.F. Eyck, Surface comparison of active and inactive protein kinases identifies a conserved activation mechanism, Proc. Natl. Acad. Sci. USA 103 (2006) 17783–17788, https://doi.org/10.1073/pnas.0607656103.
[32] A.P. Kornev, S.S. Taylor, L.F. Ten Eyck, A helix scaffold for the assembly of active protein kinases, Proc. Natl. Acad. Sci. USA 105 (2008) 14377–14382, https://doi.org/10.1073/pnas.0807988105.
[33] H.S. Meharena, P. Chang, M.M. Keshwani, K. Oruganty, A.K. Nene, N. Kannan, S. S. Taylor, A.P. Kornev, Deciphering the structural basis of eukaryotic protein kinase regulation, PLoS Biol. 11 (2013) e1001690, https://doi.org/10.1371/journal.pbio.1001680.
[34] R. Roskoski Jr., Classification of small molecule protein kinase inhibitors based upon the structures of their drug-enzyme complexes, Pharm. Res 103 (2016) 26–48, https://doi.org/10.1016/j.phrs.2015.10.021.
[35] R. Roskoski Jr., The ErbB/HER family of protein-tyrosine kinases and cancer, Pharm. Res. 79 (2014) 34–74, https://doi.org/10.1016/j.phrs.2013.11.002.
[36] R. Roskoski Jr., ErbB/HER protein-tyrosine kinases: structure and small molecule inhibitors, Pharm. Res 87 (2014) 42–59, https://doi.org/10.1016/j.phrs.2014.06.001.
[37] R. Roskoski Jr., Small molecule inhibitors targeting the EGFR/ErbB family of protein-tyrosine kinases in human cancers, Pharm. Res. 139 (2019) 395–411, https://doi.org/10.1016/j.phrs.2018.11.014.
[38] R. Roskoski Jr., Anaplastic lymphoma kinase (ALK): structure, oncogenic activation, and pharmacological inhibition, Pharm. Res 68 (2013) 68–94, https://doi.org/10.1016/j.phrs.2012.11.007.
[39] R. Roskoski Jr., Anaplastic lymphoma kinase (ALK) inhibitors in the treatment of ALK-driven lung cancers, Pharm. Res. 117 (2017) 343–356, https://doi.org/10.1016/j.phrs.2017.01.007.
[40] R. Roskoski Jr., The preclinical profile of crizotinib in the treatment of non-small cell lung cancer and other neoplastic disorders, Expert Opin. Drug Dis. 8 (2013) 1165–1179, https://doi.org/10.1517/17460441.2013.813015.
[41] R. Roskoski Jr., The role of fibroblast growth factor receptor (FGFR) protein-tyrosine kinase inhibitors in the treatment of cancers including those of the urinary bladder, Pharm. Res. 151 (2020) 104567, https://doi.org/10.1016/j.phrs.2019.104567.
[42] R. Roskoski Jr., The role of small molecule platelet-derived growth factor receptor (PDGFR) inhibitors in the treatment of neoplastic disorders, Pharm. Res. 129 (2018) 65–83, https://doi.org/10.1016/j.phrs.2018.01.021.

[43] R. Roskoski Jr., A. Sadeghi-Nejad, Role of RET protein-tyrosine kinase inhibitors in the treatment RET-driven thyroid and lung cancers, Pharm. Res. 128 (2018) 1–17, https://doi.org/10.1016/j.phrs.2017.12.021.
[44] R. Roskoski Jr., The role of small molecule Kit protein-tyrosine kinase inhibitors in the treatment of neoplastic disorders, Pharm. Res. 133 (2018) 35–52, https://doi.org/10.1016/j.phrs.2018.04.020.
[45] R. Roskoski Jr., The role of small molecule Flt3 receptor protein-tyrosine kinase inhibitors in the treatment of Flt3-positive acute myelogenous leukemias, Pharm. Res. 155 (2020) 104725, https://doi.org/10.1016/j.phrs.2020.104725.
[46] R. Roskoski Jr., ROS1 protein-tyrosine kinase inhibitors in the treatment of ROS1 fusion protein-driven non-small cell lung cancers, Pharm. Res. 121 (2017) 202–212, https://doi.org/10.1016/j.phrs.2017.04.022.
[47] R. Roskoski Jr., Vascular endothelial growth factor (VEGF) and VEGF receptor inhibitors in the treatment of renal cell carcinomas, Pharm. Res. 120 (2017) 116–132, https://doi.org/10.1016/j.phrs.2017.03.010.
[48] R. Roskoski Jr., Janus kinase (JAK) inhibitors in the treatment of inflammatory and neoplastic diseases, Pharm. Res. 111 (2016) 784–803, https://doi.org/10.1016/j.phrs.2016.07.038.
[49] R. Roskoski Jr., Janus kinase (JAK) inhibitors in the treatment of neoplastic and inflammatory disorders, Pharm. Res. 183 (2022) 106362, https://doi.org/10.1016/j.phrs.2022.106362.
[50] R. Roskoski Jr., Ibrutinib inhibition of Bruton protein-tyrosine kinase (BTK) in the treatment of B cell neoplasms, Pharm. Res. 113 (2016) 395–408, https://doi.org/10.1016/j.phrs.2016.09.011.
[51] R. Roskoski Jr., Src protein-tyrosine kinase structure, mechanism, and small molecule inhibitors, Pharm. Res. 94 (2015) 9–25, https://doi.org/10.1016/j.phrs.2015.01.003.
[52] M.C. Frame, R. Roskoski Jr., Src family tyrosine kinases. Reference Module in Life Sciences, Elsevier, Amsterdam, 2017, pp. 1–11, https://doi.org/10.1016/B978-0-12-809633-8.07199-5.
[53] R. Roskoski Jr., Targeting BCR-Abl in the treatment of Philadelphia-chromosome positive chronic myelogenous leukemia, Pharm. Res. 178 (2022) 106156, https://doi.org/10.1016/j.phrs.2022.106156.
[54] R. Roskoski Jr., Allosteric MEK1/2 inhibitors including cobimetanib and trametinib in the treatment of cutaneous melanomas, Pharm. Res. 117 (2017) 20–31, https://doi.org/10.1016/j.phrs.2016.12.009.
[55] R. Roskoski Jr., Cyclin-dependent protein kinase inhibitors including palbociclib as anticancer drugs, Pharm. Res. 107 (2016) 249–275, https://doi.org/10.1016/j.phrs.2016.03.012.
[56] R. Roskoski Jr., ERK1/2 MAP kinases: structure, function, and regulation, Pharm. Res. 66 (2012) 105–143, https://doi.org/10.1016/j.phrs.2012.04.005.
[57] R. Roskoski Jr., Targeting ERK1/2 protein-serine/threonine kinases in human cancers, Pharm. Res. 142 (2019) 151–168, https://doi.org/10.1016/j.phrs.2019.01.039.
[58] A. Martin-Vega, M.H. Cobb, Navigating the ERK1/2 MAPK Cascade, Biomolecules 13 (2023) 1555, https://doi.org/10.3390/biom13101555.
[59] R. Roskoski Jr., Targeting oncogenic Raf protein-serine/threonine kinases in human cancers, Pharm. Res. 135 (2018) 239–258, https://doi.org/10.1016/j.phrs.2018.08.013.
[60] R. Roskoski Jr., RAF protein-serine/threonine kinases: structure and regulation, Biochem Biophys. Res. Commun. 399 (2010) 313–317, https://doi.org/10.1016/j.bbrc.2010.07.092.
[61] Y. Liu, K. Shah, F. Yang, L. Witucki, K.M. Shokat, A molecular gate which controls unnatural ATP analogue recognition by the tyrosine kinase v-Src, Bioorg. Med. Chem. 6 (1998) 1219–1226, https://doi.org/10.1016/s0968-0896(98)00099-6.
[62] A.C. Dar, K.M. Shokat, The evolution of protein kinase inhibitors from antagonists to agonists of cellular signaling, Annu Rev. Biochem 80 (2011) 769–795, https://doi.org/10.1146/annurev-biochem-090308-173656.
[63] P.M. Ung, R. Rahman, A. Schlessinger, Redefining the protein kinase conformational space with machine learning, Cell Chem. Biol. 25 (2018) 916–924.e2, https://doi.org/10.1016/j.chembiol.2018.05.002.
[64] R. Hu, H. Xu, P. Jia, Z. Zhao, KinaseMD: kinase mutations and drug response database, Nucleic Acids Res. 49 (D1) (2021) D552–D561, https://doi.org/10.1093/nar/gkaa945.
[65] R. Roskoski Jr., A historical overview of protein kinases and their targeted small molecule inhibitors, Pharm. Res. 100 (2015) 1–23, https://doi.org/10.1016/j.phrs.2015.07.010.
[66] D. Fabbro, S.W. Cowan-Jacob, H. Moebitz, Ten things you should know about protein kinases: IUPHAR Review 14, Br. J. Pharm. 172 (2015) 2675–2700, https://doi.org/10.1111/bph.13096.
[67] A.J. Kooistra, A. Volkamer, Kinase-centric computational drug development, Ann. Rep. Med. Chem. 50 (2017) 197–236, https://doi.org/10.1016/bs.armc.2017.08.001.
[68] M. Malumbres, M. Barbacid, RAS oncogenes: the first 30 years, Nat. Rev. Cancer 3 (2003) 459–465, https://doi.org/10.1038/nrc1097.
[69] A.G. Stephen, D. Esposito, R.K. Bagni, F. McCormick, Dragging Ras back in the ring, Cancer Cell 25 (2014) 272–281, https://doi.org/10.1016/j.ccr.2014.02.017.
[70] D.K. Simanshu, D.V. Nissley, F. McCormick, RAS proteins and their regulators in human disease, Cell 170 (2017) 17–33, https://doi.org/10.1016/j.cell.2017.06.009.
[71] M. Holderfield, M.M. Deuker, F. McCormick, M. McMahon, Targeting RAF kinases for cancer therapy: BRAF-mutated melanoma and beyond, Nat. Rev. Cancer 14 (2014) 455–467, https://doi.org/10.1038/nrc3760.
[72] G.M. Nitulescu, G. Stancov, O.C. Seremet, G. Nitulescu, D.P. Mihai, C.G. Duta-Bratu, S.F. Barbuceanu, O.T. Olaru, The importance of the pyrazole scaffold in the design of protein kinases inhibitors as targeted anticancer therapies, Molecules 28 (2023) 5359, https://doi.org/10.3390/molecules28145359.
[73] M.A. Hossain, A comprehensive review of targeting RAF kinase in cancer, Eur. J. Pharm. 986 (2025) 177142, https://doi.org/10.1016/j.ejphar.2024.177142.
[74] E.H. Chang, M.A. Gonda, R.W. Ellis, E.M. Scolnick, D.R. Lowy, Human genome contains four genes homologous to transforming genes of Harvey and Kirsten murine sarcoma viruses, Proc. Natl. Acad. Sci. USA 79 (1982) 4848–4852, https://doi.org/10.1073/pnas.79.16.4848.
[75] G.M. Cooper, Cellular transforming genes, Science 217 (1982) 801–806, https://doi.org/10.1126/science.6285471.
[76] N.K. Williams, R.S. Bamert, O. Patel, C. Wang, P.M. Walden, A.F. Wilks, et al., Dissecting specificity in the Janus kinases: the structures of JAK-specific inhibitors complexed to the JAK1 and JAK2 protein tyrosine kinase domains, J. Mol. Biol. 387 (2009) 219–232, https://doi.org/10.1016/j.jmb.2009.01.041.
[77] A.F. Wilks, The JAK kinases: not just another kinase drug discovery target, Semin Cell Dev. Biol. 19 (2008) 319–328, https://doi.org/10.1016/j.semcdb.2008.07.020.
[78] M. Kawamura, D.W. McVicar, J.A. Johnston, T.B. Blake, Y.Q. Chen, B.K. Lal, A. R. Lloyd, D.J. Kelvin, J.E. Staples, J.R. Ortaldo, J.J. O'Shea, Molecular cloning of L-JAK, a Janus family protein-tyrosine kinase expressed in natural killer cells and activated leukocytes, Proc. Natl. Acad. Sci. USA 91 (1994) 6374–6378, https://doi.org/10.1073/pnas.91.14.6374.
[79] R. Roskoski Jr., Deucravacitinib is an allosteric TYK2 protein kinase inhibitor FDA-approved for the treatment of psoriasis, Pharm. Res 189 (2023) 106642, https://doi.org/10.1016/j.phrs.2022.106642.
[80] J.J. Babon, I.S. Lucet, J.M. Murphy, N.A. Nicola, L.N. Varghese, The molecular regulation of Janus kinase (JAK) activation, Biochem J. 462 (2014) 1–13, https://doi.org/10.1042/BJ20140712.
[81] S. Abroun, N. Saki, M. Ahmadvand, F. Asghari, F. Salari, F. Rahim, STATs: an old story, yet mesmerizing, Cell J. 17 (2015) 395–411, https://doi.org/10.22074/cellj.2015.1.
[82] X. Chen, U. Vinkemeier, Y. Zhao, D. Jeruzalmi, J.E. Darnell Jr., J. Kuriyan, Crystal structure of a tyrosine phosphorylated STAT-1 dimer bound to DNA, Cell 93 (1998) 827–839, https://doi.org/10.1016/s0092-8674(00)81443-9.
[83] F. Zuccotto, E. Ardini, E. Casale, M. Angiolini, Through the "gatekeeper door": exploiting the active kinase conformation, J. Med. Chem. 53 (2010) 2691–2694, https://doi.org/10.1021/jm901443h.
[84] L.K. Gavrin, E. Saiah, Approaches to discover non-ATP site inhibitors, Med. Chem. Commun. 4 (2013) 41–51, https://doi.org/10.1039/C2MD20180A.
[85] V. Lamba, I. Ghosh, New directions in targeting protein kinases: focusing upon true allosteric and bivalent inhibitors, Curr. Pharm. Des. 18 (2012) 2936–2945, https://doi.org/10.2174/138161212800672813.
[86] J.J. Liao, Molecular recognition of protein kinase binding pockets for design of potent and selective kinase inhibitors, J. Med Chem. 50 (2007) 409–424, https://doi.org/10.1021/jm0608107.
[87] O.P. van Linden, A.J. Kooistra, R. Leurs, I.J. de Esch, C. de Graaf, KLIFS: a knowledge-based structural database to navigate kinase-ligand interaction space, J. Med Chem. 57 (2014) 249–277, https://doi.org/10.1021/jm400378w.
[88] A.J. Kooistra, G.K. Kanev, O.P. van Linden, R. Leurs, I.J. de Esch, C. de Graaf, KLIFS: a structural kinase-ligand interaction database, Nucleic Acids Res. 44 (D1) (2016) D365–D371, https://doi.org/10.1093/nar/gkv1082.
[89] G.K. Kanev, C. de Graaf, B.A. Westerman, I.J.P. de Esch, A.J. Kooistra, KLIFS: an overhaul after the first 5 years of supporting kinase research, Nucleic Acids Res. (2020) gkaa895, https://doi.org/10.1093/nar/gkaa895.
[90] B. Wienen-Schmidt, D. Schmidt, H.D. Gerber, A. Heine, H. Gohlke, G. Klebe, Surprising non-additivity of methyl groups in drug-kinase interaction, ACS Chem. Biol. 14 (2019) 2585–2594, https://doi.org/10.1021/acschembio.9b00476.
[91] D. Bajusz, G.G. Ferenczy, G.M. Keserű, Structure-based virtual screening approaches in kinase-directed drug discovery, Curr. Top. Med. Chem. 17 (2017) 2235–2259, https://doi.org/10.2174/1568026617666170224121313.
[92] P. Wu, T.E. Nielsen, M.H. Clausen, FDA-approved small-molecule kinase inhibitors, Trends Pharm. Sci. 36 (2015) 422–439, https://doi.org/10.1016/j.tips.2015.04.005.
[93] K.B. Patel, D.E. Heppner, Lazertinib: breaking the mold of third-generation EGFR inhibitors, RSC Med Chem. (2025), https://doi.org/10.1039/d4md00800f.
[94] D.E. Heppner, F. Wittlinger, T.S. Beyett, T. Shaurova, D.A. Urul, B. Buckley, C. D. Pham, I.K. Schaeffner, B. Yang, B.C. Ogboo, E.W. May, E.M. Schaefer, M.J. Eck, S.A. Laufer, P.A. Hershberger, Structural basis for inhibition of mutant EGFR with lazertinib (YH25448), ACS Med Chem. Lett. 13 (2022) 1856–1863, https://doi.org/10.1021/acsmedchemlett.2c00213.
[95] D.E. Heppner, F. Wittlinger, T.S. Beyett, T. Shaurova, D.A. Urul, B. Buckley, C. D. Pham, I.K. Schaeffner, B. Yang, B.C. Ogboo, E.W. May, E.M. Schaefer, M.J. Eck, S.A. Laufer, P.A. Hershberger, Structural basis for inhibition of mutant EGFR with lazertinib (YH25448), ACS Med Chem. Lett. 13 (2022) 1856–1863, https://doi.org/10.1021/acsmedchemlett.2c00213.
[96] M. Bergoug, M. Doudeau, F. Godin, C. Mosrin, B. Vallée, H. Bénédetti, Neurofibromin structure, functions and regulation, Cells 9 (2020) 2365, https://doi.org/10.3390/cells9112365.
[97] R.E. Strowd 3rd, Available therapies for patients with neurofibromatosis-related nervous system tumors, Curr. Treat. Options Oncol. 21 (2020) 81, https://doi.org/10.1007/s11864-020-00779-z.
[98] T.O. Fischmann, C.K. Smith, T.W. Mayhood, J.E. Myers, P. Reichert, A. Mannarino, D. Carr, H. Zhu, J. Wong, R.S. Yang, H.V. Le, V.S. Madison, Crystal structures of MEK1 binary and ternary complexes with nucleotides and inhibitors, Biochemistry 48 (2009) 2661–2674, https://doi.org/10.1021/bi801898e.

[99] Z.M. Khan, A.M. Real, W.M. Marsiglia, A. Chow, M.E. Duffy, J.R. Yerabolu, A. P. Scopton, A.C. Dar, Structural basis for the action of the drug trametinib at KSR-bound MEK, Nature 588 (2020) 509–514, https://doi.org/10.1038/s41586-020-2760-4.
[100] S. Dhillon, Tovorafenib: first approval, Drugs 84 (2024) 985–993, https://doi.org/10.1007/s40265-024-02069-6.
[101] S. Singh, D. Bradford, S. Chatterjee, X. Li, S.L. Aungst, A.M. Skinner, C.P. Miller, S. Kim-McOlash, J. Fourie Zirkelbach, Y. Xiong, Y. Bi, Y.H. Wang, Y. Yang, J. Sun, J. Kraft, R. Charlab, S.S. Shord, S. Tang, B. Scepura, I. Bulatao, O. Udoka, H. Saber, N.A. Rahman, R. Pazdur, H. Singh, M. Donoghue, N. Drezner, FDA approval summary: tovorafenib for relapsed or refractory BRAF-altered pediatric low-grade glioma, Clin. Cancer Res. (2025), https://doi.org/10.1158/1078-0432.CCR-24-3439.
[102] C.M. van Tilburg, L.B. Kilburn, S. Perreault, R. Schmidt, A.A. Azizi, O. Cruz-Martínez, M. Zápotocký, K. Scheinemann, A.Y.N.S. Meeteren, A. Sehested, E. Opocher, P.H. Driever, S. Avula, D.S. Ziegler, D. Capper, A. Koch, F. Sahm, J. Qiu, L.P. Tsao, S.C. Blackman, P. Manley, T. Milde, R. Witt, D.T.W. Jones, D. Hargrave, O. Witt, LOGGIC/FIREFLY-2: a phase 3, randomized trial of tovorafenib vs. chemotherapy in pediatric and young adult patients with newly diagnosed low-grade glioma harboring an activating RAF alteration, BMC Cancer 24 (2024) 147, https://doi.org/10.1186/s12885-024-11820-x.
[103] E. Tkacik, K. Li, G. Gonzalez-Del Pino, B.H. Ha, J. Vinals, E. Park, T.S. Beyett, M. J. Eck, Structure and RAF family kinase isoform selectivity of type II RAF inhibitors tovorafenib and naporafenib, J. Biol. Chem. 299 (2023) 104634, https://doi.org/10.1016/j.jbc.2023.104634.
[104] A.K. Gupta, T. Wang, S. Polla Ravi, M.A. Bamimore, V. Piguet, A. Tosti, Systematic review of newer agents for the management of alopecia areata in adults: Janus kinase inhibitors, biologics and phosphodiesterase-4 inhibitors, J. Eur. Acad. Dermatol. Venereol. 37 (2023) 666–679, https://doi.org/10.1111/jdv.18810.
[105] I. Chim, R. Ghiya, R.D. Sinclair, S. Eisman, Novel investigational drugs for alopecia areata and future perspectives, Expert Opin. Invest. Drugs 33 (2024) 441–449, https://doi.org/10.1080/13543784.2024.2348062.
[106] M.H. Fitzhugh, J.G. Hansen, A. Jabbari, K.G. Berrebi, Pathophysiology of Alopecia Areata in the Pediatric Patient, Pedia Dermatol. 42 1 (1) (2025) 24–30, https://doi.org/10.1111/pde.15842.
[107] T. Dainichi, M. Iwata, Y. Kaku, Alopecia areata: What's new in the diagnosis and treatment with JAK inhibitors? J. Dermatol. (2023) https://doi.org/10.1111/1346-8138.17064.
[108 T. Passeron, B. King, J. Seneschal, M. Steinhoff, A. Jabbari, M. Ohyama, D.J. Tobin, S. Randhawa, A. Winkler, J.B. Telliez, D. Martin, A. Lejeune, Inhibition of T-cell activity in alopecia areata: recent developments and new directions, Front Immunol. 14 (2023) 1243556, https://doi.org/10.3389/fimmu.2023.1243556.
[109] A.K. Gupta, S.P. Ravi, K. Vincent, W. Abramovits, LITFULO™ (Ritlecitinib) capsules: a Janus kinase 3 Inhibitor for the treatment of severe alopecia areata, Skinmed 21 (2023) 434–438, eCollection 2023.
[110] L. Horn, J.R. Infante, K.L. Reckamp, G.R. Blumenschein, T.A. Leal, S.N. Waqar, B. J. Gitlitz, R.E. Sanborn, J.G. Whisenant, L. Du, J.W. Neal, J.P. Gockerman, G. Dukart, K. Harrow, C. Liang, J.J. Gibbons, A. Holzhausen, C.M. Lovly, H. A. Wakelee, Ensartinib (X-396) in ALK-positive non-small cell lung cancer: results from a first-in-human phase I/II, multicenter study, Clin. Cancer Res 24 (12) (2018) 2771–2779, https://doi.org/10.1158/1078-0432.CCR-17-2398.
[111] R.L. Siegel, T.B. Kratzer, A.N. Giaquinto, H. Sung, A. Jemal, Cancer statistics, 2025, CA Cancer J. Clin. 75 (2025) 10–45, https://doi.org/10.3322/caac.21871.
[112] R. Roskoski Jr., Targeted and cytotoxic inhibitors used in the treatment of lung cancers, Pharm. Res 209 (2024) 107465, https://doi.org/10.1016/j.phrs.2024.107465.
[113] J.J. Cui, M. McTigue, M. Nambu, M. Tran-Dubé, M. Pairish, H. Shen, L. Jia, H. Cheng, J. Hoffman, P. Le, M. Jalaie, G.H. Goetz, K. Ryan, N. Grodsky, Y. L. Deng, M. Parker, S. Timofeevski, B.W. Murray, S. Yamazaki, S. Aguirre, Q. Li, H. Zou, J. Christensen, Discovery of a novel class of exquisitely selective mesenchymal-epithelial transition factor (c-MET) protein kinase inhibitors and identification of the clinical candidate 2-(4-(1-(quinolin-6-ylmethyl)-1H-[1,2,3]triazolo[4,5-*b*]pyrazin-6-yl)-1H-pyrazol-1-yl)ethanol (PF-04217903) for the treatment of cancer, J. Med. Chem. 55 (2012) 8091–8109, https://doi.org/10.1021/jm300967g.
[114] D. Ma, M. Guo, X. Zhai, An updated patent review of anaplastic lymphoma kinase inhibitors (2018-2022), Expert Opin. Ther. Pat. 33 (2023) 323–337, https://doi.org/10.1080/13543776.2023.2216381.
[115] J. Zheng, T. Wang, Y. Yang, J. Huang, J. Feng, W. Zhuang, J. Chen, J. Zhao, W. Zhong, Y. Zhao, Y. Zhang, Y. Song, Y. Hu, Z. Yu, Y. Gong, Y. Chen, F. Ye, S. Zhang, L. Cao, Y. Fan, G. Wu, Y. Guo, C. Zhou, K. Ma, J. Fang, W. Feng, Y. Liu, Z. Zheng, G. Li, H. Wang, S. Cang, N. Wu, W. Song, X. Liu, S. Zhao, L. Ding, G. Selvaggi, Y. Wang, S. Xiao, Q. Wang, Z. Shen, J. Zhou, J. Zhou, L. Zhang, Updated overall survival and circulating tumor DNA analysis of ensartinib for crizotinib-refractory ALK-positive NSCLC from a phase II study, Cancer Commun. 44 (2024) 455–468, https://doi.org/10.1002/cac2.12524.
[116] L. Mastrantoni, G. Giordano, E. Vita, G. Horn, J. Russo, A. Orlandi, G. Daniele, D. Giannarelli, G. Tortora, E. Bria, The likelihood of being helped or harmed as a patient-centred tool to assess ALK-Inhibitors clinical impact and safety in ALK-addicted non-small cell lung cancer: a systematic review and sensitivity-analysis, Cancer Treat. Res. Commun. 41 (2024) 100842, https://doi.org/10.1016/j.ctarc.2024.100842.
[117] R. Roskoski Jr., Rule of five violations among the FDA-approved small molecule protein kinase inhibitors, Pharm. Res. 191 (2023) 106774, https://doi.org/10.1016/j.phrs.2023.106774.
[118] C.A. Lipinski, F. Lombardo, B.W. Dominy, P.J. Feeney, Experimental and computational approaches to estimate solubility and permeability in drug discovery and development settings, Adv. Drug Deliv. Rev. 46 (2001) 3–26, https://doi.org/10.1016/s0169-409x(00)00129-0.
[119] A.L. Hopkins, C.R. Groom, A. Alex, Ligand efficiency: a useful metric for lead selection, Drug Discov. Today 9 (2004) 430–431, https://doi.org/10.1016/S1359-6446(04)03069-7.
[120] P.D. Leeson, B. Springthorpe, The influence of drug-like concepts on decision-making in medicinal chemistry, Nat. Rev. Drug Discov. 6 (2007) 881–890, https://doi.org/10.1038/nrd2445.
[121] T.W. Johnson, R.A. Gallego, M.P. Edwards, Lipophilic efficiency as an important metric in drug design, J. Med. Chem. 61 (2018) 6401–6420, https://doi.org/10.1021/acs.jmedchem.8b00077.
[122] A.L. Hopkins, G.M. Keserü, P.D. Leeson, D.C. Rees, C.H. Reynolds, The role of ligand efficiency metrics in drug discovery, Nat. Rev. Drug Discov. 13 (2014) 105–121, https://doi.org/10.1038/nrd4163.
[123] P.D. Leeson, Molecular inflation, attrition, and the rule of five, Adv. Drug Deliv. Rev. 101 (2016) 22–33, https://doi.org/10.1016/j.addr.2016.01.018.
[124] D.F. Veber, S.R. Johnson, H.Y. Cheng, B.R. Smith, K.W. Ward, K.D. Kopple, Molecular properties that influence the oral bioavailability of drug candidates, J. Med. Chem. 45 (2002) 2615–2623, https://doi.org/10.1021/jm020017n.
[125] T.I. Oprea, Property distribution of drug-related chemical databases, J. Comput. Aided Mol. Des. 14 (2000) 251–264, https://doi.org/10.1023/a:1008130001697.
[126] P.D. Leeson, A.P. Bento, A. Gaulton, A. Hersey, E.J. Manners, C.J. Radoux, A. R. Leach, Target-based evaluation of "drug-like" properties and ligand efficiencies, J. Med. Chem. 64 (2021) 7210–7230, https://doi.org/10.1021/acs.jmedchem.1c00416.
[127] S.H. Bertz, The first general index of molecular complexity, J. Am. Chem. Soc. 1103 (1981) 3559–3601.
[128] J.B. Hendrickson, P. Huang, A.G. Toczko, Molecular complexity: a simplified formula adapted to individual atoms, J. Chem. Inf. Comput. Sci. 27 (1987) 63–67.
[129] T.J. Ritchie, S.J. Macdonald, Physicochemical descriptors of aromatic character and their use in drug discovery, J. Med. Chem. 57 (2014) 7206–7215, https://doi.org/10.1021/jm500515d.
[130] M.K. Bayliss, J. Butler, P.L. Feldman, D.V. Green, P.D. Leeson, M.R. Palovich, A. J. Taylor, Quality guidelines for oral drug candidates: dose, solubility and lipophilicity, Drug Discov. Today 21 (2016) 1719–1727, https://doi.org/10.1016/j.drudis.2016.07.007.
[131] T.I. Oprea, C.G. Bologa, S. Brunak, A. Campbell, G.N. Gan, A. Gaulton, S. M. Gomez, R. Guha, A. Hersey, J. Holmes, A. Jadhav, L.J. Jensen, G.L. Johnson, A. Karlson, A.R. Leach, A. Ma'ayan, A. Malovannaya, S. Mani, S.L. Mathias, M. T. McManus, T.F. Meehan, C. von Mering, D. Muthas, D.T. Nguyen, J. P. Overington, G. Papadatos, J. Qin, C. Reich, B.L. Roth, S.C. Schürer, A. Simeonov, L.A. Sklar, N. Southall, S. Tomita, I. Tudose, O. Ursu, D. Vidovic, A. Waller, D. Westergaard, J.J. Yang, G. Zahoránszky-Köhalmi, Unexplored therapeutic opportunities in the human genome, Nat. Rev. Drug Discov. 17 (2018) 377, https://doi.org/10.1038/nrd.2018.52.
[132] L. Huang, S. Jiang, Y. Shi, Tyrosine kinase inhibitors for solid tumors in the past 20 years (2001-2020), J. Hematol. Oncol. 13 (2020) 143, https://doi.org/10.1186/s13045-020-00977-0.
[133] K. Bechman, M. Yates, J.B. Galloway, The new entries in the therapeutic armamentarium: the small molecule JAK inhibitors, Pharm. Res. 147 (2019) 104392, https://doi.org/10.1016/j.phrs.2019.104392. Corrigendum doi: 10.1016/j.phrs.2020.104634.
[134] M.A. Adas, E. Alveyn, E. Cook, M. Dey, J.B. Galloway, K. Bechman, The infection risks of JAK inhibition, Expert Rev. Clin. Immunol. 18 (2022) 253–261, https://doi.org/10.1080/1744666X.2022.2014323.
[135] R. Roskoski Jr., Cost in the United States of FDA-approved small molecule protein kinase inhibitors used in the treatment of neoplastic and non-neoplastic diseases, Pharm. Res. 199 (2023) 107036, https://doi.org/10.1016/j.phrs.2023.107036.
[136] C.I. Wells, H. Al-Ali, D.M. Andrews, C.R.M. Asquith, A.D. Axtman, I. Dikic, D. Ebner, P. Ettmayer, C. Fischer, M. Frederiksen, R.E. Futrell, N.S. Gray, S. B. Hatch, S. Knapp, U. Lücking, M. Michaelides, C.E. Mills, S. Müller, D. Owen, A. Picado, K.S. Saikatendu, M. Schröder, A. Stolz, M. Tellechea, B.J. Turunen, S. Vilar, J. Wang, W.J. Zuercher, T.M. Willson, D.H. Drewry, The kinase chemogenomic set (KCGS): an open science resource for kinase vulnerability identification, Int. J. Mol. Sci. 22 (2021) 566, https://doi.org/10.3390/ijms22020566.
[137] J. Choo, G. Heo, C. Pothoulakis, E. Im, Posttranslational modifications as therapeutic targets for intestinal disorders, Pharm. Res. (2021) 105412, https://doi.org/10.1016/j.phrs.2020.105412.
[138] C.C. Ayala-Aguilera, T. Valero, Á. Lorente-Macías, D.J. Baillache, S. Croke, A. Unciti-Broceta, Small molecule kinase inhibitor drugs (1995-2021): medical indication, pharmacology, and synthesis, J. Med. Chem. 65 (2022) 1047–1131, https://doi.org/10.1021/acs.jmedchem.1c00963.
[139] Z. Xie, X. Yang, Y. Duan, J. Han, C. Liao, Small-molecule kinase inhibitors for the treatment of nononcologic diseases, J. Med. Chem. 64 (2021) 1283–1345, https://doi.org/10.1021/acs.jmedchem.0c01511.
[140] R. Roskoski Jr., Blockade of mutant RAS oncogenic signaling with a special emphasis on KRAS, Pharm. Res. 172 (2021) 105806, https://doi.org/10.1016/j.phrs.2021.105806.
[141] A. Cichońska, B. Ravikumar, R.J. Allaway, F. Wan, S. Park, O. Isayev, S. Li, M. Mason, A. Lamb, Z. Tanoli, M. Jeon, S. Kim, M. Popova, S. Capuzzi, J. Zeng, K. Dang, G. Koytiger, J. Kang, C.I. Wells, T.M. Willson, IDG-DREAM Drug-Kinase Binding Prediction Challenge Consortium, T.I. Oprea, A. Schlessinger, D. H. Drewry, G. Stolovitzky, K. Wennerberg, J. Guinney, T. Aittokallio,

Crowdsourced mapping of unexplored target space of kinase inhibitors, Nat. Commun. 12 (2021) 3307, https://doi.org/10.1038/s41467-021-23165-1.
[142] H.Y. Min, H.Y. Lee, Molecular targeted therapy for anticancer treatment, Exp. Mol. Med. (2022), https://doi.org/10.1038/s12276-022-00864-3.
[143] X. Lu, J.B. Smaill, K. Ding, New promise and opportunities for allosteric kinase inhibitors, Angew. Chem. Int. Ed. Engl. 59 (2020) 13764–13776, https://doi.org/10.1002/anie.201914525.
[144] R. Roskoski Jr., Combination immune checkpoint and targeted protein kinase inhibitors for the treatment of renal cell carcinomas, Pharm. Res. 203 (2024) 107181, https://doi.org/10.1016/j.phrs.2024.107181.
[145] R. Roskoski Jr., Targeted and cytotoxic inhibitors used in the treatment of breast cancer, Pharm. Res 210 (2024) 107534, https://doi.org/10.1016/j.phrs.2024.107534.
[146] K. Sasaki, S.S. Strom, S. O'Brien, E. Jabbour, F. Ravandi, M. Konopleva, G. Borthakur, N. Pemmaraju, N. Daver, P. Jain, S. Pierce, H. Kantarjian, J. E. Cortes, Relative survival in patients with chronic-phase chronic myeloid leukaemia in the tyrosine-kinase inhibitor era: analysis of patient data from six prospective clinical trials, Lancet Haematol. 2 (2015) e186–e193, https://doi.org/10.1016/S2352-3026(15)00048-4.
[147] H.M. Kantarjian, N. Jain, G. Garcia-Manero, M.A. Welch, F. Ravandi, W. G. Wierda, E.J. Jabbour, The cure of leukemia through the optimist's prism, Cancer 128 (2022) 240–259, https://doi.org/10.1002/cncr.33933.
[148] E. Jabbour, H. Kantarjian, J. Cortes, Use of second- and third-generation tyrosine kinase inhibitors in the treatment of chronic myeloid leukemia: an evolving treatment paradigm, Clin. Lymphoma Myeloma Leuk. 15 (2015) 323–334, https://doi.org/10.1016/j.clml.2015.03.006.
[149] J. Cortes, C. Pavlovsky, S. Saußele, Chronic myeloid leukemia, Lancet 398 (2021) 1914–1926, https://doi.org/10.1016/S0140-6736(21)01204-6.
[150] F.G. Haddad, K. Sasaki, G.C. Issa, G. Garcia-Manero, F. Ravandi, T. Kadia, J. Cortes, M. Konopleva, N. Pemmaraju, Y. Alvarado, M. Yilmaz, G. Borthakur, C. DiNardo, N. Jain, N. Daver, N.J. Short, E. Jabbour, H. Kantarjian, Treatment-free remission in patients with chronic myeloid leukemia following the discontinuation of tyrosine kinase inhibitors, Am. J. Hematol. 97 (2022) 856–864, https://doi.org/10.1002/ajh.26550.
[151] E. Jabbour, H. Kantarjian, Chronic myeloid leukemia: a review, JAMA (2025), https://doi.org/10.1001/jama.2025.0220.
[152] R. Macarron, M.N. Banks, D. Bojanic, D.J. Burns, D.A. Cirovic, T. Garyantes, D. V. Green, R.P. Hertzberg, W.P. Janzen, J.W. Paslay, U. Schopfer, G. S. Sittampalam, Impact of high-throughput screening in biomedical research, Nat. Rev. Drug Discov. 10 (2011) 188–195, https://doi.org/10.1038/nrd3368.
[153] R.J. Young, S.L. Flitsch, M. Grigalunas, P.D. Leeson, R.J. Quinn, N.J. Turner, H. Waldmann, The time and place for nature in drug discovery, JACS Au 2 (2022) 2400–2416, https://doi.org/10.1021/jacsau.2c00415.
[154] I.V. Hartung, B.R. Huck, A. Crespo, Rules were made to be broken, Nat. Rev. Chem. (2023), https://doi.org/10.1038/s41570-022-00451-0.
[155] R. Roskoski Jr., Guidelines for preparing color figures for everyone including the colorblind, Pharm. Res. 119 (2017) 240–241, https://doi.org/10.1016/j.phrs.2017.02.005. Erratum in: Pharmacol Res 2019;139:569. doi: 10.1016/j.phrs.2018.09.019.